OXFORD

Human Molecular Genetics, 2018, Vol. 27, No. 14 2425–2442

doi: 10.1093/hmg/ddy142
Advance Access Publication Date: 20 April 2018
Original Article

ORIGINAL ARTICLE

Pre-clinical symptoms of SBMA may not be androgen-dependent: implications from two SBMA mouse models

Youfen Xu[1], Katherine Halievski[1], Masahisa Katsuno[2], Hiroaki Adachi[3], Gen Sobue[2], S. Marc Breedlove[1] and Cynthia L. Jordan[1,*]

[1]Neuroscience Program, Michigan State University, East Lansing, MI 48824, USA, [2]Department of Neurology, Nagoya University Graduate School of Medicine, Showa-ku, Nagoya 466-8550, Japan and [3]Department of Neurology, University of Occupational and Environment Health School of Medicine, Yahatanishi-ku, Kitakyushu Fukuoka 807-8555, Japan

*To whom correspondence should be addressed at: Neuroscience Program, Michigan State University, 108 Giltner Hall, 293 Farm Lane, East Lansing, MI 48824, USA. Tel: +1 5174321674; Fax: +1 5174322744; Email: jordancy@msu.edu

Abstract

A distinguishing aspect of spinal and bulbar muscular atrophy (SBMA) is its androgen-dependence, possibly explaining why only males are clinically affected. This disease, which impairs neuromuscular function, is linked to a polyglutamine expansion mutation in the androgen receptor (AR). In mouse models of SBMA, motor dysfunction is associated with pronounced defects in neuromuscular transmission, including defects in evoked transmitter release (quantal content, QC) and fiber membrane excitability (based on the resting membrane potential, RMP). However, whether such defects are androgen-dependent is unknown. Thus, we recorded synaptic potentials intracellularly from adult muscle fibers of transgenic (Tg) AR97Q male mice castrated pre-symptomatically. Although castration largely protects both QC and the RMP of fibers, correlating with the protective effect of castration on motor function, significant deficits in QC and RMP remained. Surprisingly, comparable defects in QC and RMP were also observed in *pre-symptomatic* AR97Q males, indicating that such defects emerge early and are pre-clinical. Exposing asymptomatic Tg females to androgens also induces both motor dysfunction and comparable defects in QC and RMP. Notably, asymptomatic Tg females also showed significant deficits in QC and RMP, albeit less severe, supporting their pre-clinical nature, but also raising questions about the androgen-dependence of pre-clinical symptoms. In summary, current evidence indicates that disease progression depends on androgens, but early pathogenic events may be triggered by the mutant AR allele independent of androgens. Such early, androgen-independent disease mechanisms may also be relevant to females carrying the SBMA allele.

Introduction

Spinal and bulbar muscular atrophy (SBMA), or Kennedy's disease, is a hereditary neuromuscular disorder linked to a CAG/polyglutamine expansion mutation in the first exon of the *androgen receptor* (*AR*) gene. This mutation leads to androgen-dependent loss of motor function (1,2). Only adult men are clinically affected, exhibiting proximal limb and bulbar muscle weakness and atrophy, whereas women carrying the mutant AR may experience subclinical symptoms of muscle cramping and fasciculations but without overt muscle atrophy

Received: January 5, 2018. **Revised:** March 14, 2018. **Accepted:** April 16, 2018

(3). Although SBMA has traditionally been viewed as a motor neuropathy, driven by AR toxicity in the motoneurons, recent evidence from patients and mouse models suggests that skeletal muscle is a key contributor to disease pathogenesis (4–8).

Numerous lines of evidence indicate that expression of disease symptoms depend not only on the disease-causing AR allele but also on male levels of androgens (4,9). Thus, castration of male mice carrying the disease allele, either at puberty or as adults, can rescue them from disease. Likewise, asymptomatic transgenic (Tg) females express the disease when exposed to male levels of testosterone (T) (5,10). Moreover, other interventions that lower AR expression and/or its activation have also been shown to rescue mice from symptoms of disease (4,6,11,12).

Neuromuscular junctions (NMJs) are often a pathological target for neuromuscular diseases including spinal muscular atrophy (SMA), amyotrophic lateral sclerosis, and recently demonstrated for SBMA (9,13,14). Indeed, NMJs of chronically diseased SBMA male mice are profoundly affected, both morphologically and functionally, with NMJs being highly fragmented (11,15,16) and exhibiting notable defects in evoked transmitter release and acetylcholine receptor (AChR) mRNA expression. The resting membrane potential (RMP) of diseased muscle fibers is also significantly decreased (17). Given that three different genetic mouse models of SBMA exhibit these same defects, humans with SBMA likely suffer them too.

We now ask two key questions: (1) are defects in neurotransmission androgen-dependent and (2) do such defects emerge early in the disease process? Answering the first question is essential for linking androgen-dependent motor dysfunction to the critical underlying cellular mechanisms. We answered the first question by removing testicular androgens from juvenile AR97Q mice that globally express the human mutant AR allele (10), and used intracellular recording and real-time PCR to determine whether castration can rescue synaptic and muscle function and expression of key muscle genes underlying motor dysfunction. We also exposed asymptomatic AR97Q Tg females and Tg females from the myogenic model of SBMA, in which wild-type (WT) AR is expressed at high levels only in muscle fibers, to male levels of androgens, to determine whether comparable defects in neurotransmission and muscle gene expression can be acutely induced by androgens in Tg females, like motor dysfunction itself. Despite differences in the disease allele (WT versus CAG-expanded AR) and patterns of expression (muscle-specific versus global), both the myogenic and AR97Q models exhibit remarkably similar disease phenotypes that are male-biased and androgen-dependent (5,10). Studying the myogenic model begins to shed light on whether proximate events of disease are triggered by muscle AR. To answer whether defects occur early, we also examined neurotransmission and muscle gene expression in young, pre-symptomatic AR97Q males.

We now report that defects in neuromuscular transmission are androgen-dependent like motor dysfunction itself. Castration of AR97Q males largely reversed the defects in evoked neurotransmitter release and RMP of muscle fibers, as well as reversed disease-related changes in muscle gene expression. Likewise, both acutely diseased myogenic and AR97Q females showed defects in evoked transmitter release and muscle fiber RMP comparable with that of chronically diseased males. Furthermore, androgen treatment also similarly affected muscle gene expression in acutely diseased females, leading to the pathological expression of the same genes as seen in chronically diseased males. However, castrated asymptomatic AR97Q Tg males nonetheless exhibited residual defects in function and gene expression as symptomatic AR97Q males do. Importantly, comparable defects were found in asymptomatic Tg females as well as pre-symptomatic juvenile AR97Q males, raising the possibility that early defects underlying pre-clinical symptoms may *not* be androgen-dependent. Such defects may be necessary but not sufficient to cause overt motor dysfunction.

Results

Castration rescues synaptic and motor function in AR97Q Tg males

We began by asking whether pre-pubertal castration of pre-symptomatic AR97Q Tg male mice (ages 30–32 days) would prevent synaptic and muscle dysfunction, comparable with its beneficial effect on motor function. Pre-symptomatic stage was judged on the basis of the hang test, a 2-min test of their capacity to hang on to a metal grid in an upside-down position. We found that AR97Q mice performed equivalent to WT males at ages 33–40 days, showing maximal time on the hang test, and thus were considered 'pre-symptomatic' (Tables 1 and 2). As previously reported (17), pre-pubertal castration fully protected the motor function of AR97Q Tg male mice, with adult AR97Q males castrated pre-pubertally (Tg + C) performing at WT levels on the hang test (Fig. 1A) as opposed to age-matched gonadally intact AR97Q males who showed profound deficits in hang times (Tg + S) (Fig. 1A, Tg + C versus Tg + S: $P = 0.008$). The sparing of motor function was also accompanied by significant protection of the RMP of muscle fibers and neuromuscular transmission in the fast-twitch extensor digitorum longus (EDL) muscle (Fig. 1B–J). In particular, the low RMP of muscle fibers in diseased AR97Q males was largely reversed by early castration (Fig. 1B, Tg + S versus Tg + C: $P < 0.001$). However, the RMP of fibers was also significantly lower in asymptomatic castrated Tg (Tg + C versus WT + C: $P < 0.001$). Although endplate potential (EPP) amplitude did not significantly differ across groups (Fig. 1C), miniature endplate potential (mEPP) amplitude did (Fig. 1D), with diseased junctions in gonadally intact Tg males (Tg + S) having larger mEPP amplitudes than all other groups, indicated by the rightward shift in the cumulative frequency distribution. This shift was fully reversed by early castration of AR97Q males (Tg + C versus Tg + S: $P < 0.015$; Tg + C versus WT + C: $P = 0.86$, on the basis of Kolmogorov–Smirnov test). Likewise, the disease-related deficit in evoked quantal content (QC) was largely rescued by pre-pubertal castration of AR97Q males (Fig. 1E), with a significant increase in QC compared with symptomatic Tg controls (Tg + C versus Tg + S: $P < 0.001$). However, like the RMP, there was a significant residual deficit in QC in castrated asymptomatic Tg males (Tg + C versus WT + C: $P = 0.016$) despite their normal performance on the hang test. Although the frequency of spontaneous release was not significantly affected by disease or castration (data not shown), decay times were. Castration prevented the prolonged decay times of both mEPPs and EPPs (Fig. 1F–H), suggesting that castration also prevented the disease-related changes in the expression of AChR subunits (17), as we later confirmed (Fig. 2). Similarly, the disease-related resistance to μ-conotoxin (μ-CTX), the sodium channel blocker used to prevent muscle contraction was reversed by castration. Muscle fiber contraction of castrated Tg males was efficiently blocked using the same concentration of μ-CTX (2.5 μM, 15–20 min incubation) as for WTs, whereas muscle from intact Tg males required a higher concentration of toxin (5 μm, incubation with more than 20 min) to achieve the

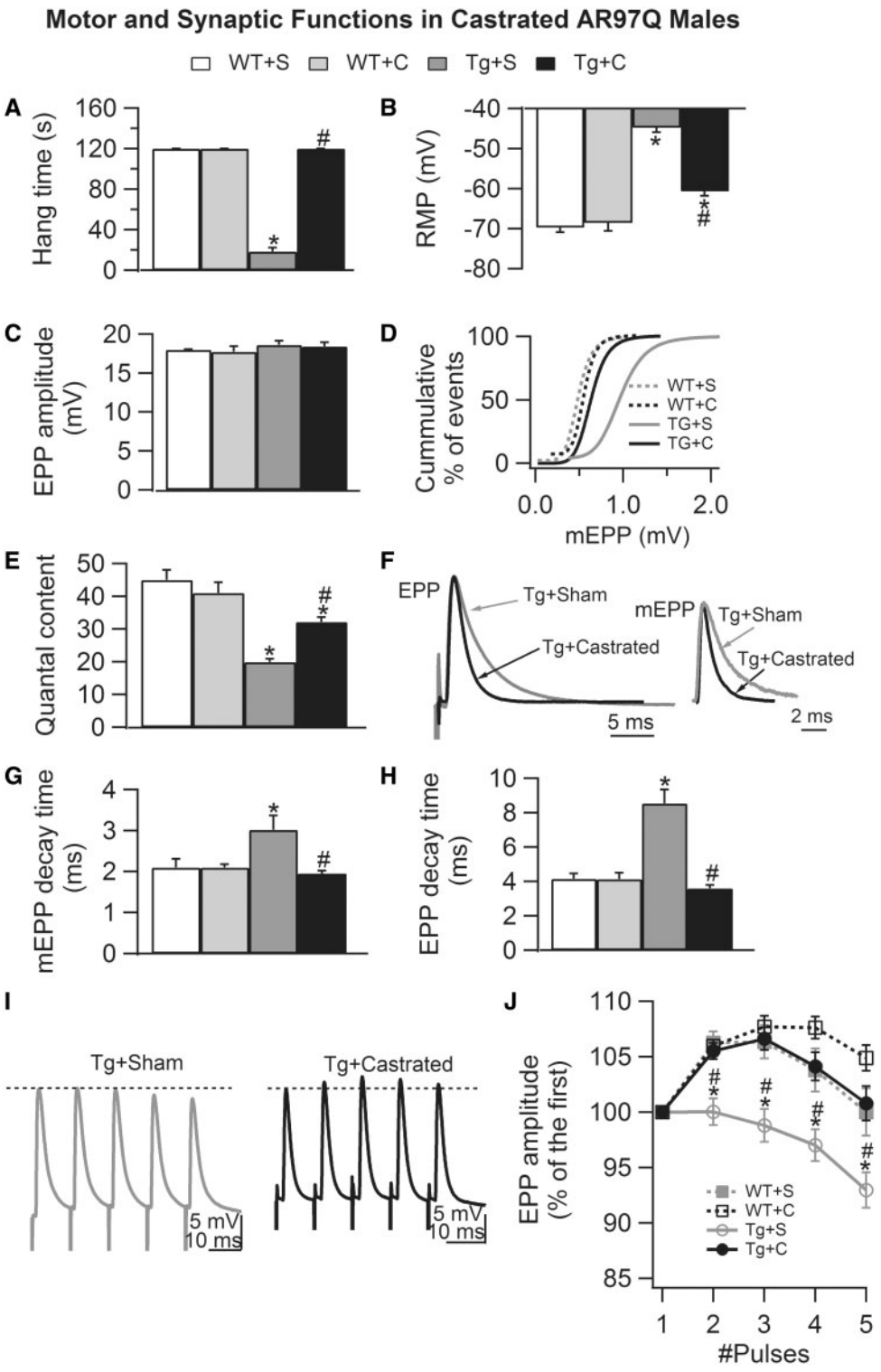

Figure 1. Castration of pre-symptomatic transgenic AR97Q males largely protects synaptic function. (**A**) Motor function based on hang times for AR97Q males was fully protected by castration pre-symptomatically, confirming previous reports. (**B**) The RMP of muscle fibers in symptomatic gonadally intact AR97Q males (Tg + S) is significantly depolarized compared with that of WT muscle fibers (WT + S, WT + C). Castrating pre-symptomatic Tg males largely reverses this effect of disease, maintaining membrane excitability at near normal in age-matched castrated Tg (Tg + C) males. Note however a small but significant residual effect on the RMP of AR97Q fibers, despite normal hang times of Tg + C males (A). This residual deficit may be related to the fact that fibers at the time of castration are already significantly depolarized (Fig. 3). Although neither disease or gonadal androgens affects EPP amplitude (**C**), the cumulative histograms of mEPP amplitude (**D**) show that disease shifts mEPPs toward significantly larger values (seen as a rightward shift in the curve), an effect prevented by castration (P values <0.05 on the basis of Kolmogorov–Smirnov test). (**E**) Likewise, disease impairs evoked transmitter release, significantly decreasing QC by more than half in gonadally intact Tg males, an effect largely but not fully prevented by castration. These data suggest that castration also rescued the size of the RRP of synaptic vesicles and/or probability of release. The residual deficit in QC in castrated Tg males may also be related to an early deficit in QC pre-symptomatically (Fig. 3). (**F**) Representative EPP (average of 10–20 responses) and mEPP traces

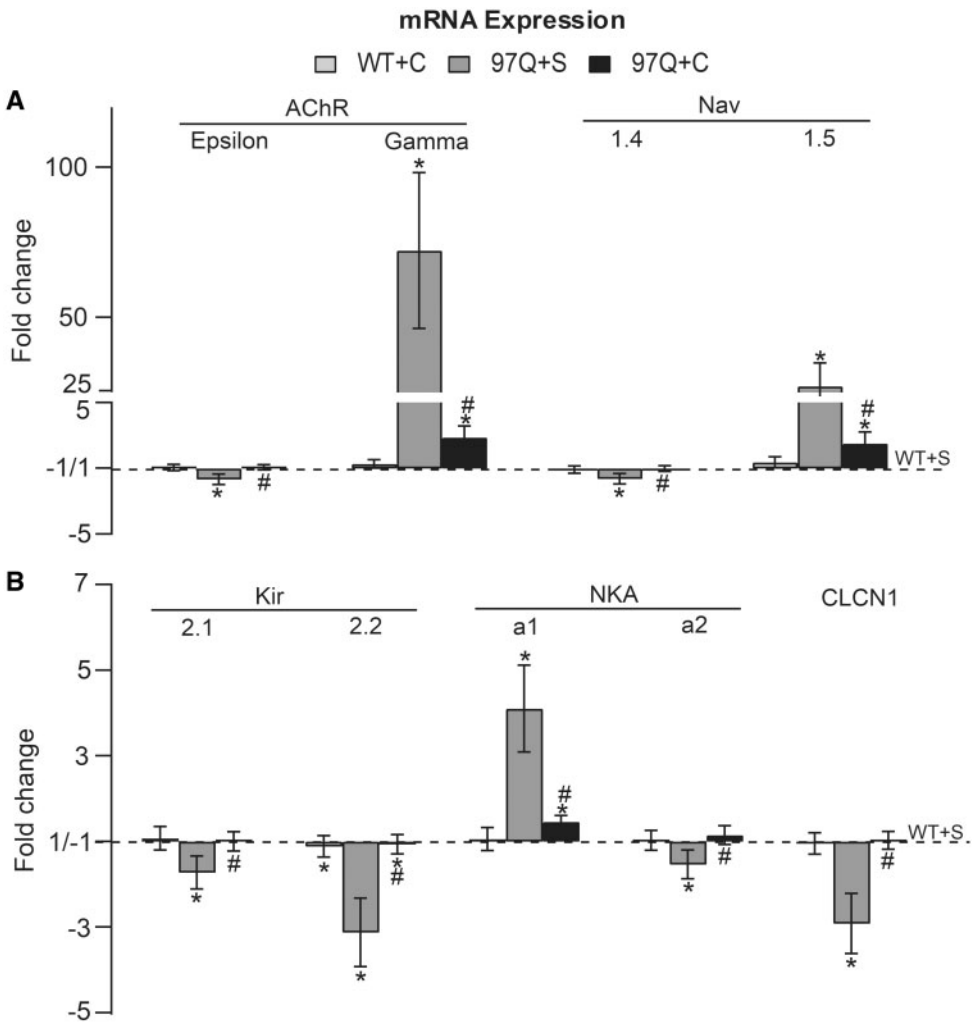

Figure 2. Pre-pubertal castration largely prevents pathological change in mRNA expression in AR97Q adult muscle. (**A**) The disease-related deficit in adult isoforms, AChR-ϵ subunit and sodium channel Nav1.4, are completely rescued by castration. Castration also largely reversed the disease-related increase in expression of mRNA for neonatal isoforms AChR-γ and Nav1.5, which underlie the slowed kinetics of EPPs and mEPPs and resistance to μ-CTX in disease, respectively. However, note small but significant increases in the expression of both AChR-γ and Nav1.5, apparently emerging sometime after castration (Fig. 3) *independent* of circulating gonadal androgens. Evidently the system can tolerate some level of pathological expression of the immature isoforms without affecting mEPP and EPP kinetics, likely reflecting which subunit (adult versus immature) predominates at any given time. (**B**) Similarly, mRNA expression for the *Clcn1*, and transcripts for the inward rectifying potassium channel (Kir2.1 and 2.2), and sodium/potassium pump (NKA a1 and a2) were all restored to normal by pre-pubertal castration of Tg males, consistent with the significant rescue of the RMP (Fig. 1). These data show that disease-related changes in the expression of muscle genes for ion channels and ion transporters underlying muscle and synaptic function are largely androgen-dependent, correlating well with the androgen-dependent loss of motor function in this SBMA model. Nonetheless, it also appears that mutant AR has the capacity to trigger subclinical symptoms of disease. Values are mean fold changes ± SEMs (standard errors of the mean) relative to WT + S values based on N/group (WT + S, WT + C and Tg + S: $N = 7$; Tg + C: $N = 8$). $^{*}P < 0.05$ from WT sham or WT castrated; $^{\#}P < 0.05$ from Tg sham. 'S' denotes sham castration; 'C' denotes castration.

same level of block. This result suggested that castration also prevented the aberrant expression of the neonatal sodium channel (17) as we later confirmed (Fig. 2). Castration also prevented the defect in short-term synaptic facilitation that is characteristic of chronically diseased junctions (Fig. 1I and J, Tg + C versus Tg + S: $P < 0.001$; Tg + C versus WT + C: $P > 0.05$).

Quantitative reverse transcriptase-polymerase chain reaction (RT-qPCR) was used to determine whether pre-pubertal

(average of 2 min recording), normalized and aligned by their peak, from castrated (black) and sham (gray)-operated Tgs reveal visibly prolonged decay times for junctions from diseased gonadally intact Tg males compared with asymptomatic castrated Tg males. (**G and H**) Averaged values confirm significant increases in both EPP and mEPP decay times for gonadally intact, motor-impaired Tg males, an effect that is completely prevented by castration of pre-symptomatic Tg males. These data suggest that the pathological expression of the gamma subunit of the AChR is also reversed, as we later confirmed (Fig. 3). (**I and J**) Castration also improves short-term synaptic facilitation in Tg males, reversing a significant disease-related deficit. Representative traces of EPPs (average of 10–20 individual EPPs evoked by trains of five pulses at 100 Hz) in sham-control (black) and castrated (gray) Tg males show that significant decreases in synaptic facilitation emerge quickly, evident even at the second pulse in diseased Tg males (J). Although castration also seemed to enhance synaptic facilitation of WT junctions, this effect was not significant. Values plotted are group means (*N* for motor function and *n* for synaptic function) ± SEM (WT sham: $n/N = 30/3$; WT castrate: $n/N = 30/3$; Tg sham: $n/N = 42/4$; Tg castrate: $n/N = 52/5$) with *n* indicating the number of endplates/mice and *N* indicating the number of mice/experimental group. $^{*}P < 0.05$ from WT sham or WT castrated EDL; $^{\#}P < 0.05$ from Tg sham EDL. 'S' denotes sham castration; 'C' denotes castration.

Table 1. Electrophysiological measures from pre-symptomatic (AR97Q males), asymptomatic (AR97Q castrated males, and AR97Q and myogenic females) and fully symptomatic mice

Electrophysiology	**Pre- or asymptomatic** Hang time = 120 s				**Symptomatic** Hang time < 30 s		
	Males		Females		Males	Females	
Models	Juvenile AR97Q	Castrated AR97Q	Control myogenic	Control AR97Q	Intact AR97Q	T-treated myogenic	T-treated AR97Q
Age (days) at time of study	33–40	63–95	80–255	64–95	63–95	80–255	64–95
n/*N*	42/4	52/5	30/3	40/4	42/4	40/4	40/4
Symptom onset (days)					63–95	5	14–17
RMP	↓*	↓*	↓*	↓*	↓*+	↓*#	↓*#
QC	↓*	↓*	–	↓*	↓*+	↓*#	↓*#
EPP amplitude	–	–	–	–	–	↓*#	–
mEPP amplitude	↑*	–	–	–	↑*+	–	↑*#
mEPP decay time	–	–	–	–	↑*+	–	↑*#
EPP decay time	–	–	–	–	↑*+	↑#	↑*#

Direction of arrow indicates direction of disease-induced change relative to WT. Significant deficits in the RMP and QC of adult diseased NMJs are also characterized in pre-symptomatic juvenile AR97Q males and asymptomatic adult AR97Q males castrated pre-symptomatically, suggesting that both measures capture pre-clinical traits of disease triggered independent of androgens. Of note, asymptomatic transgenic (Tg) females in both myogenic and AR97Q models also show the same defects independent of male levels of androgens, reinforcing the idea that some pre-clinical defects are initially triggered in the absence of ligand by a disease-causing AR acting in skeletal muscle. Defects in RMP and QC are more severely affected in fully symptomatic mice in the presence of androgens, indicating their androgen-sensitivity with disease progression. Given that prolonged mEPP and/or EPP decay times, involving a subunit switch from epsilon to gamma in the AChR, tightly correlates with the emergence of motor symptoms in both male and female mice of both models, this effect on decay time appears to mark late-stage disease. Most other presumed markers of disease do not generalize across all models and thus, may not be authentic markers of disease for SBMA in humans. ↑ Significantly altered compared with their WT controls. ↑ More severely affected compared with pre-symptomatic Tg male mice or respective asymptomatic Tg female controls.

*$P < 0.05$, compared with WT; +$P < 0.05$, compared with castrated AR97Q male; #$P < 0.05$, compared with control female. *n* is the number of endplates per experimental group and *N* is the number of mice per experiment group.

castration of AR97Q mice also rescued muscle gene expression. We found that indeed it did, largely protecting muscle gene expression from diseased-related changes. Specifically, pathological changes in mRNA expression of AChR subunits were largely prevented, reversing both the down-regulation in mRNA for the adult AChR-ϵ subunit and the up-regulation in mRNA for the immature AChR-γ subunit (Fig. 2A, Tg + C versus Tg + S: $P < 0.001$ and Tg + C versus WT + C: $P > 0.05$ for ϵ-subunit; Tg + C versus Tg + S: $P < 0.001$ and Tg + C versus WT + C: $P = 0.002$ for γ-subunit). These data align with the decay times of EPPs and mEPPs in castrated asymptomatic Tg males which are normal (Fig. 1G and H and Tables 1 and 2) (14,18). Note that a small but significant increase in the gamma subunit persists despite the normal decay times, indicating that normal expression of the ϵ-subunit is sufficient for full restoration of channel kinetics. Similarly, abnormal expression of sodium channel mRNA was largely restored; castration prevented the disease-related loss in adult Nav1.4 mRNA and largely, but not completely, prevented the pathological increase in mRNA for the immature Nav1.5 (Fig. 2A, Tg + C versus Tg + S: $P = 0.011$ and Tg + C versus WT + C: $P > 0.05$ for Nav1.4; Tg + C versus Tg + S: $P < 0.001$ and Tg + C versus WT + C: $P = 0.006$ for Nav1.5). These data align well with the recovery of normal sensitivity to μ-CTX in muscles from castrated AR97Q males. We also examined mRNA expression levels for the inward-rectifying potassium (Kir2) channel and the Na^+, K^+ATPase transport (Na^+, K^+ pump, NKA) that are essential for maintaining the RMP of skeletal muscle fibers (19). Expression of both of the most prevalent isoforms in adult skeletal muscle, Kir2.1and Kir2.2 isoforms, were significantly reduced in muscles from motor-impaired males and completely rescued by castration (Fig. 2B, Tg + C versus Tg + S: $P = 0.016$ and Tg + C versus WT + C: $P > 0.05$ for Kir2.1; Tg + C versus Tg + S: $P < 0.001$ and Tg + C versus WT + C: $P > 0.05$ for Kir2.2). Likewise, the amount of mRNA for the Na^+, K^+ pump α2 isoform, a major isoform expressed by adult skeletal muscles, was significantly less in diseased muscle compared with WTs but at WT levels in muscle from castrated AR97Q males (Fig. 2B, Tg + C versus Tg + S: $P = 0.003$ and Tg + C versus WT + C: $P > 0.05$) (20). The Na^+, K^+ pump α1 isoform, a minor isoform in skeletal muscle, was significantly up-regulated by disease, which was largely but not completely prevented by castration (Fig. 2B, Tg + C versus Tg + S: $P < 0.001$ and Tg + C versus WT + C: $P = 0.04$) (20). The increased expression of Na^+, K^+ pump α1 isoform may be a compensatory response to the loss of the α2 isoform, a response also seen in α2 knockout mice and other models of neuromuscular disease (21,22). Increased expression of α1 may offer some protection against the effects of disease on the RMP. Disease-related deficits in chloride channel gene 1 (*Clcn1*) mRNA were also fully prevented by pre-pubertal castration (Fig. 2B, Tg + C versus Tg + S: $P < 0.001$ and Tg + C versus WT + C: $P > 0.05$). In summary, these data show that the androgen-dependent loss of motor function in AR97Q SBMA mice is tightly correlated with pathological changes in muscle gene expression that control synaptic and muscle function. These functional changes are likely critical mediators of motor dysfunction as disease progresses and suggest new targets for the pharmacological rescue of function.

Neuromuscular synapses are dysfunctional in pre-symptomatic AR97Q males

We next asked whether pre-symptomatic AR97Q males (33–44 days of age) showed disease-related changes in synaptic and muscle function. The residual defects in the RMP and quantal

Table 2. mRNA expression in skeletal muscle from pre-symptomatic, asymptomatic and fully symptomatic AR97Q and/or myogenic SBMA mice

Gene expression (relative to WT)		**Pre- or asymptomatic** Hang time = 120 s				**Symptomatic** Hang time < 30 s		
		Males		Females		Males	Females	
Models		Juvenile AR97Q	Castrated AR97Q	Control myogenic	Control AR97Q	Intact AR97Q	T-treated myogenic	T-treated AR97Q
Age (days) at time of study		29–32	55–104	101–153	64–73	55–104	101–153	64–73
N		6	8	6	4	8	6	4
Symptom onset (days)						55–104	5	14–17
AChR	ε	↓*	–	↓*	–	↓*+	↓*#	↓*#
	γ	–	↑*	–	↑*	↑*+	–	↑*
Nav	1.4	↓*	–	–	–	↓*+	↓*#	–
	1.5	–	↑*	–	↑*	↑*+	↑*#	↑*
Kir	2.1	↓*	–	↓*	↓*	↓*+	↓*#	↓*#
	2.2	–	↓*	–	–	↓*+	–	↓*
NKA	α1	–	↑*	–	↑*	↑*+	↑*#	↑*
	α2	↓*	–	–	–	↓*+	–	↓*#
CLCN1		↓*	–	–	–	↓*+	↓*#	↓*#

Direction of arrow indicates direction of disease-induced change relative to WT. The adult epsilon (ε) subunit is unaltered in muscle of asymptomatic adult AR97Q males (castrated pre-symptomatically) and asymptomatic AR97Q females but is affected in muscle of pre-symptomatic AR97Q males and asymptomatic myogenic females, showing a slight, yet significant decrease. As motor symptoms emerge in the presence of adult male levels of androgen, epsilon mRNA in muscle is greatly reduced, irrespective of model and sex, suggesting that the role of androgen is to exacerbate an existing deficit triggered by mutant AR independent of ligand. The AChR neonatal isoform gamma (γ) is upregulated in muscle from both diseased and asymptomatic adult AR97Q males, a defect not evident in pre-symptomatic AR97Q males. AR97Q females, both acutely diseased and asymptomatic controls, show this same increase in gamma mRNA, with a more robust increase in gamma expression in muscle from motor-impaired AR97Q females. Gamma subunit is unaffected in myogenic females. Together, these data indicate that AChR is a target of disease in SBMA contributing to synaptic dysfunction. mRNA levels for the adult Nav1.4 of the voltage-dependent sodium channel in muscle is somewhat reduced in pre-symptomatic AR97Q males but unaffected in all other groups of asymptomatic Tg mice. As motor impairments emerge, Nav1.4 mRNA becomes markedly reduced in both AR97Q males and myogenic females, but not in symptomatic AR97Q females. The neonatal isoform Nav1.5 is robustly upregulated in muscle of both symptomatic AR97Q and myogenic mice and asymptomatic AR97Q control females and adult AR97Q males castrated pre-symptomatically. These data indicate that the effect is not fully dependent on androgens. Kir2.1 mRNA encoding the *Kcnj2* gene for the inward rectifying potassium channel shows a small but significant deficit in muscle of pre-symptomatic males and asymptomatic females. This deficit increases as motor symptoms emerge, suggesting that Kir2.1 expression level marks disease progression. Kir2.2 is reduced only in the AR97Q model. NKA α1 transcript encoding *Atp1a1* gene for the sodium/potassium pump shows nearly the same pattern of change as AChR gamma, with small but significant increases in muscle from asymptomatic adult AR97Q mice (but not myogenic), with robust upregulation in the three symptomatic groups. NKAα2 is reduced only in the AR97Q model, indicating that this and the effect on Kir2.2 may depend on an expanded polyglutamine repeat in AR. *Clcn1* transcripts are is slightly reduced in pre-symptomatic AR97Q young males and unaltered in other asymptomatic mice, but robustly and uniformly reduced in symptomatic mice of both models. This defect may be depend exclusively on androgen in SBMA because it emerges only in the present of androgens and is fully reversed in muscle of asymptomatic adult AR97Q males castrated pre-symptomatically. In summary, down-regulation of adult isoforms AChR epsilon subunit, Kir2.1 and *Clcn1* and up-regulation of neonatal isoform Nav1.5 and NKA α1 consistently occur in both chronic and acutely symptomatic SBMA models, although these same genes are less altered or unaltered in pre- or asymptomatic models. These data suggest that such biomarkers are readout of androgen–dependent progression of disease in SBMA. Reduced Kir2.1 levels may be a good pre-clinical biomarker, because it could be readily examined in muscle biopsies and would shed light on the degree of muscle fiber depolarization and hence, muscle dysfunction.

↑Significantly altered compared with their WT controls. ↑More altered compared with their pre-symptomatic mice.

*$P < 0.05$ from WT; +$P < 0.05$ from castrated AR97Q male; #$P < 0.05$ from blank-treated female. *N* is the number of mice per experiment group.

release in asymptomatic adult AR97Q mice castrated prepubertally suggested that such defects might emerge early and precede the loss of motor function. Pre-symptomatic AR97Q males have normal body weight and motor function (Fig. 3A and B). We were therefore surprised to find that both the RMP of muscle fibers and evoked QC were as severely affected in pre-symptomatic males as in chronically diseased adult males, with a 20 mV depolarization in the RMP (Fig. 3C, $P < 0.001$) and a 32% deficit in evoked QC (Fig. 3F, $P < 0.001$). These data indicate that defects in fiber excitability and evoked transmitter release occur

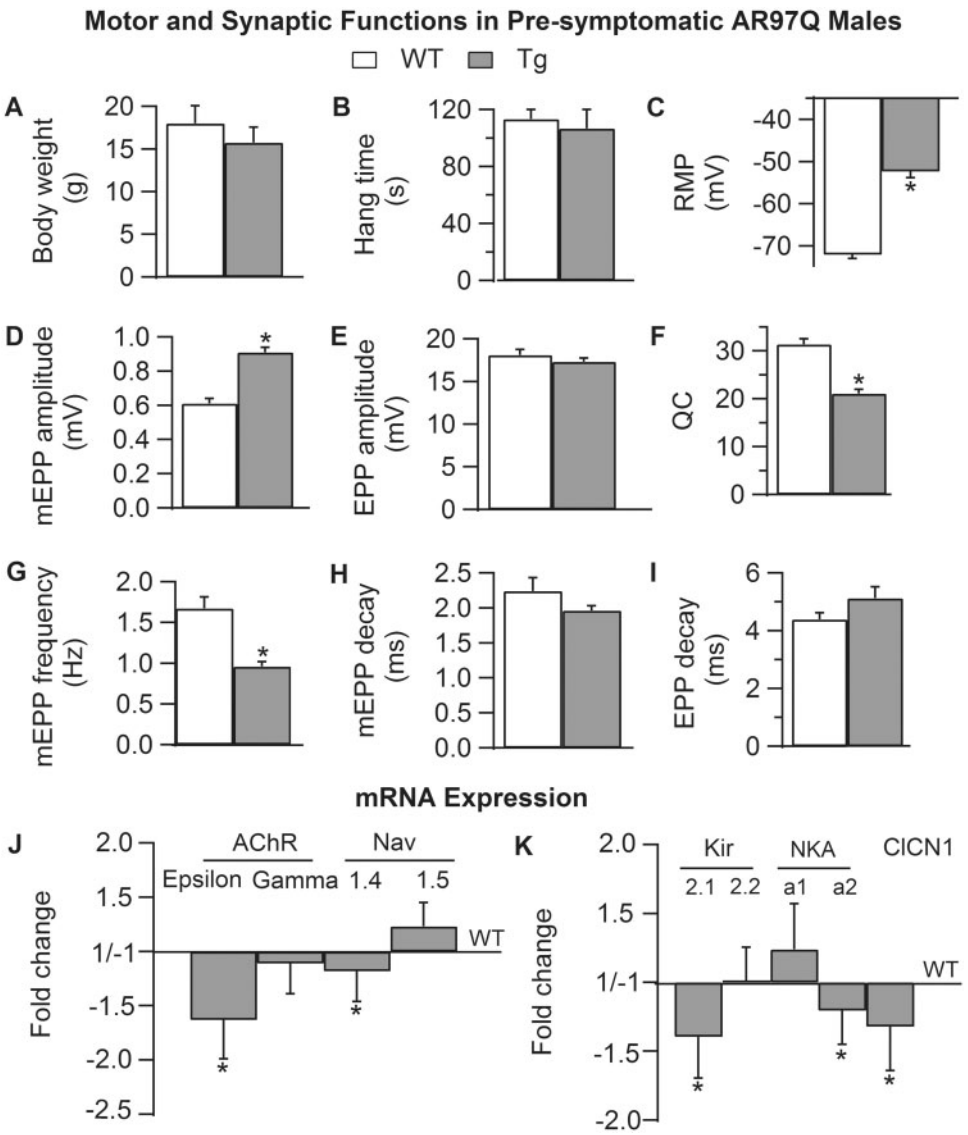

Figure 3. Neuromuscular synapses are defective in pre-symptomatic AR97Q males. (**A** and **B**) Body weight and motor function based on hang time is normal in 33- to 40-day-old AR97Q males. (**C**) However, the RMP of muscle fibers of pre-symptomatic Tg males is already significantly depolarized compared with age-matched WT males, comparable with that of late-stage diseased Tg males (Fig. 1). We also find that quantal size (mEPP amplitude) is significantly larger than normal (**D**) but EPP amplitude is not similarly affected (**E**), causing a significant deficit in QC (**F**) in pre-symptomatic males, also comparable with late-stage, motor impaired AR97Q males (Fig. 1). (**G**) Spontaneous release of transmitter (mEPP frequency) is also significantly decreased in pre-symptomatic AR97Q mice compared with WT males. (**H** and **I**) Unlike diseased adults, the decay time of mEPPs and EPPs is not altered in pre-symptomatic AR97Q NMJs. (**J** and **K**) Quantitative (q) PCR revealed that the expression of several critical genes is perturbed in muscle of pre-symptomatic AR97Q males, despite the lack of detectable motor dysfunction. Expression of the embryonic AChR γ-subunit is normal in Tg mice, as expected given the normal decay time of synaptic potentials. However, mRNA for the adult ε-subunit is significantly decreased, indicating an effect of disease already on this measure (**J**). Likewise, expression of the adult isoform of the sodium channel (Nav1.4) is significantly reduced, as in late-stage muscle, but without the increase in mRNA for the neonatal isoform (Nav1.5) that eventually renders diseased fiber in AR97Q adults appreciably less sensitive to μ-CTX. Expression of the adult isoform of the chloride channel is significantly decreased in pre-symptomatic AR97Q males (**K**), comparable with late-stage muscle. As expected based on the ∼20 mV depolarizing shift in the RMP, we find defects in the expression of both the inward rectifier potassium channel (Kir2) and the sodium/potassium pump (NKA), two critical determinants of the RMP of skeletal muscle fibers. Both Kir2.1 and NKA α2 mRNAs are significantly downregulated in muscle of pre-symptomatic AR97Q males, whereas Kir2.2 and NKA a1 mRNA levels are unaltered. These data identify several putative pre-clinical markers of disease that represent novel therapeutic targets for halting disease before irreparable damage is done. Findings also begin to characterize the sequelae of pathogenic events that underlie the progressive loss of motor ability. For example, loss of adult isoforms evidently precede, and possibly trigger, the upregulation of neonatal isoforms. A–I: Values plotted are group means (*N* for motor function and *n* for synaptic function) ± SEM (WT: $n/N = 42/4$; pre-symptomatic AR97Q: $n/N = 42/4$) normalized to WT values with *n* indicating the number of endplates/mice and *N* the number of mice per experimental group from the fast twitch EDL muscle. J and K: Values are mean fold changes ± SEMs based on *N*/group (AR97Q: $N = 6$; WT: $N = 8$) from the fast twitch anterior tibialis muscle. *$P < 0.05$ from WT.

early, before symptom onset. Although EPP amplitude was not affected (Fig. 3E, $P = 0.31$), mean quantal size on the basis of mEPP amplitude was, being 150% larger than that of WTs (Fig. 3D, $P < 0.001$). mEPP frequency was also reduced by 43%, in pre-symptomatic NMJs compared with WTs (Fig. 3G, $P < 0.001$). We did not however find effects on either mEPP or EPP decay times (Fig. 3H and I, $P > 0.05$) nor on the sensitivity to μ-CTX (data not shown) as found in muscle from symptomatic, late-stage AR97Q males (17). These data suggest that the disease-related expression of immature isoforms AChR γ-subunit and

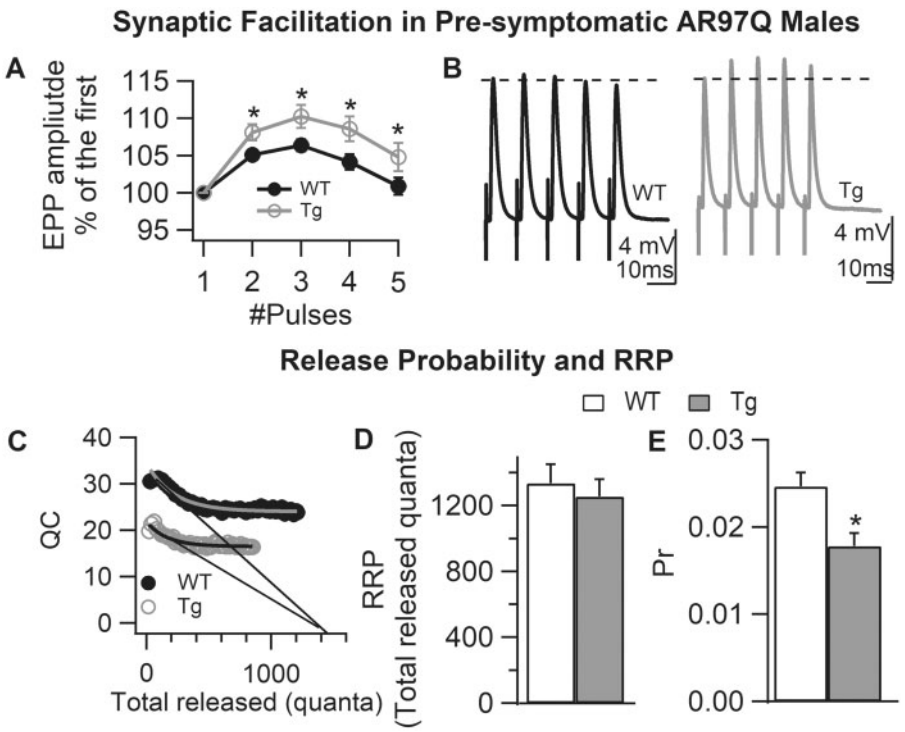

Figure 4. Reduced probability of transmitter release underlies enhanced short-term synaptic facilitation in pre-symptomatic AR97Q NMJs. (**A**) Synapses in pre-symptomatic AR97Q males exhibit a significant increase in facilitation (based on average EPP responses to trains of five pulses at 100 Hz) compared with junctions from WT males of the same age, suggesting a reduced probability of transmitter release. (**B**) Representative traces of evoked EPP (average of 10–20 individual EPPs) from WT and pre-symptomatic AR97Q NMJs showing the enhanced size of EPPs with repeated stimulation for Tg junctions. (**C** and **D**) The size of the RRP for pre-symptomatic AR97Q males is unaffected (C). The same *x*-intercept extrapolated from the initial phase of rapid decline in QC for Tg and WT synapses indicates that the maximum number of immediately releasable quanta (RRP size) without replenishment is comparable, with mean (± SEM) values in (D). (**E**) Pr, on the other hand, is significantly decreased in motor nerve terminals of pre-symptomatic AR97Q males, indicating that early deficits in QC reflect deficits in Pr with the size of the RRP eventually also reduced as disease progresses. Pr was calculated as initial QC/RRP. Values plotted are group means ± SEM (WT: $n/N = 42/4$ and pre-symptomatic AR97Q: $n/N = 42/4$). *n* is the number of endplates per experimental group and *N* is the number of mice per experimental group. *$P < 0.05$ from WT.

Nav1.5 Na channels might not be characteristic of muscles from pre-symptomatic AR97Q males. Indeed, our RT-qPCR results show no evidence of either isoform (neonatal isoforms of AChR γ-subunit and the voltage-gated sodium channel Nav1.5) being affected in pre-symptomatic AR97Q muscles (Fig. 3J). However, expression of adult isoforms for each subunit were significantly reduced, by 1.6-fold for AChR ϵ-subunit ($P = 0.012$) and 1.2-fold ($P = 0.041$) for Nav1.4 (Fig. 3J). Interestingly, the severity of these defects in the asymptomatic juveniles was nearly comparable with that of symptomatic adult AR97Q males (1.4-fold reduction for AChR ϵ-subunit and 1.7-fold for Nav1.4) (17). mRNA expression for both the inward-rectifying potassium (Kir2) ion channel and Na^+, K^+ ATPase transport (Na^+, K^+ pump, NKA) was also affected in pre-symptomatic muscle (Fig. 3K). Kir2.1 isoform was marginally significantly reduced ($P = 0.051$) with no effects on Kir2.2 whereas the adult Na^+, K^+ pump α2 isoform was significantly reduced in muscle of pre-symptomatic AR97Q male compared with age-matched WT controls ($P = 0.022$). The α1 isoform was not significantly altered. mRNA expression for the adult chloride channel was significantly reduced in pre-symptomatic males ($P = 0.021$), but the magnitude of the effect was about half that of end-stage AR97Q males. These data suggest that defects in mRNA expression for Kir2 and the Na^+, K^+ pump, and possibly the chloride channel, underlie the depolarized resting state of muscle fibers in pre-symptomatic AR97Q males, and that these are pre-clinical markers of disease that precede the emergence of overt motor dysfunction.

We also found that short-term synaptic facilitation was enhanced pre-symptomatically in AR97Q males (Fig. 4A and B, $P < 0.05$), consistent with the deficit in QC. To determine what mechanisms were behind these changes, we estimated the size of the readily releasable pool (RRP) and release probability (Pr), and found that the RRP size was unaltered in pre-symptomatic mice, but Pr was significantly decreased (Fig. 4C–E). These data indicate that the deficit in QC and increased short-term synaptic facilitation in pre-symptomatic AR97Q mice is caused by a deficit in Pr.

Exogenous androgen induces comparable defects in synaptic and muscle function in acutely diseased females

To further investigate the androgen dependence of synaptic dysfunction in SBMA, we treated adult asymptomatic Tg female mice with T to acutely induce disease. These experiments were conducted on mice from two models, the myogenic model where transgenic AR is expressed only in skeletal muscle, and the AR97Q model, where transgenic AR is globally expressed. Because Tg females display motor dysfunction only when exposed to male levels of androgen, they offer a unique opportunity to dissociate secondary effects of chronic disease from primary mechanisms that directly affect function. Myogenic Tg females also allow us to evaluate whether muscle AR *per se* is responsible for the disease-related changes observed. If muscle

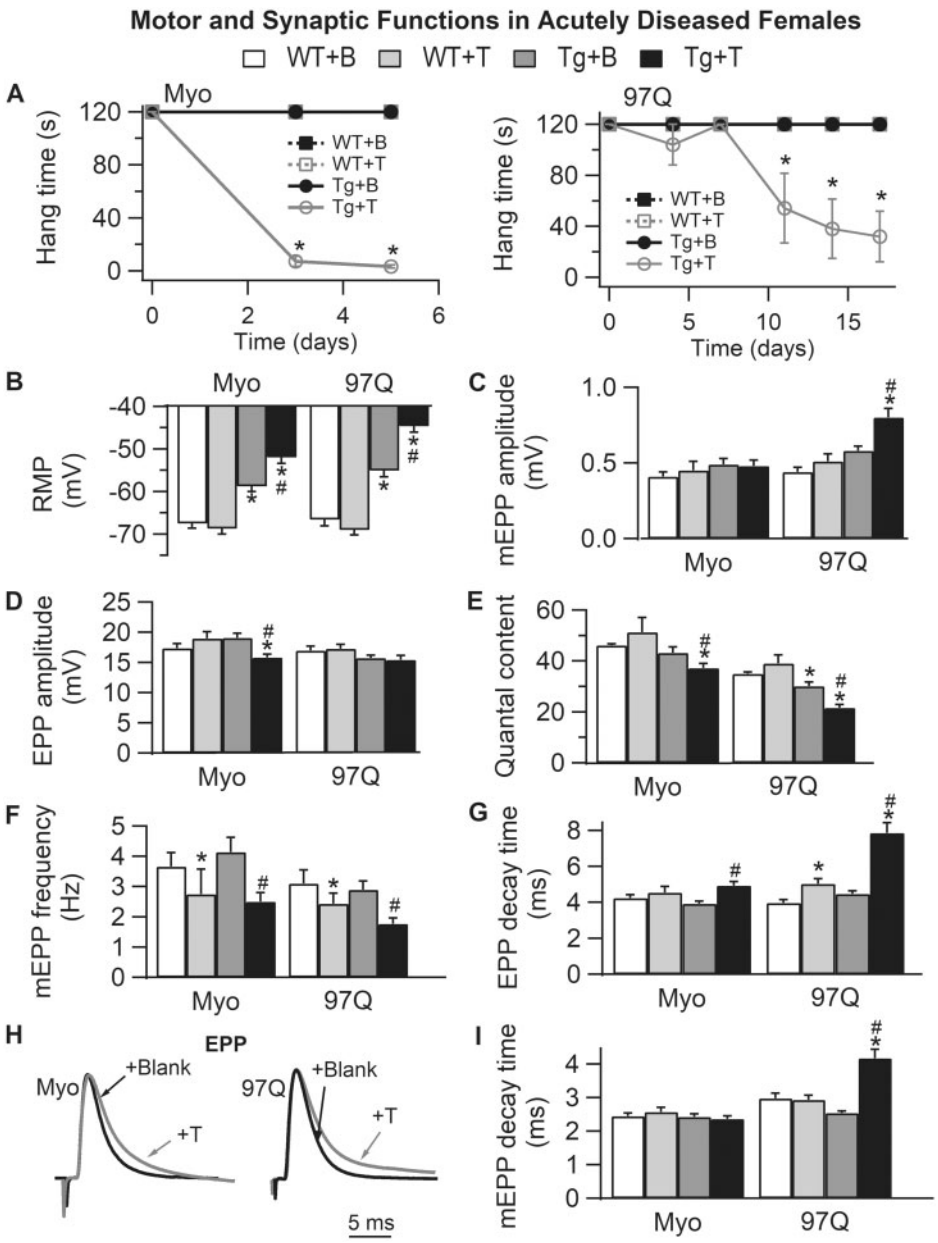

Figure 5. Acute androgen treatment induces comparable synaptic and motor dysfunction in two female models of SBMA, the myogenic (Myo) and AR97Q models. (**A**) Only 5 days of testosterone treatment drives rapid loss of motor function in myogenic females (expressing WT androgen receptor only in muscle fibers), whereas androgen-dependent demise of motor function in AR97Q females takes a full 2 weeks. (**B**) The RMP of EDL muscle fibers is significantly depolarized in testosterone (T)-treated females of both models, comparable with that of diseased males. Note that the RMP in asymptomatic blank (B)-treated Tg females in both models is also significantly depolarized compared with WT controls, akin to that of pre-symptomatic AR97Q males (Fig. 3). These data indicate that muscle fibers in SBMA models are diseased prior to overt motor dysfunction and *i*ndependent of male levels of androgens. T has no such effect on the RMP of WT fibers. (**C**) Only junctions in diseased AR97Q females show significant increases in mEPP amplitude triggered by T, comparable with that of symptomatic AR97Q males (Fig. 3). (**D**) On the other hand, EPP amplitude is significantly *reduced* by T treatment in myogenic females. (**E**) The net effect of T on the size of EPPs and mEPPs in the two models is a significant reduction in QC for symptomatic Tg females of both models. Also note that QC is significantly reduced in asymptomatic AR97Q females, again mirroring defects observed in pre-symptomatic AR97Q males. These data also underscore the possibility that some effects of mutant AR may be independent of androgens. Moreover, synaptic weakening is likely a core trait of SBMA that begins early and precedes overt motor dysfunction. (**F**) Androgen treatment also reduced mEPP frequency, although this effect does not depend on the disease-causing transgene, because T also has comparable effects in WTs, suggesting that this effect is not a product of disease. (**G–I**) T prolongs decay time of EPPs (G and H) in both Tg models, correlating with motor dysfunction, and comparable with chronically diseased males in both models. This defect may mark the progression of disease from asymptomatic to symptomatic, because it is not evident in asymptomatic Tg females nor in pre-symptomatic AR97Q males (Fig. 3). Representative average EPP traces from both T-treated (gray) and B-treated (black) Tg females which have been normalized and aligned by their peak to compare decay rates (H). Note that although mEPP decay time (I) is prolonged only in T-treated AR97Q females, T prolongs EPP decay time (G) for diseased junctions of *both* myogenic and AR97Q females. We also find that T treatment induced a slight, but significant prolongation of EPP decay in WT control females after two weeks of treatment but not after five days (WTs for AR97Q model versus WTs for myogenics), indicating that T can also affect EPP kinetics in WT muscle. These data show that although considerable pathology in synaptic and muscle functions is driven by the *combination* of androgens and a disease allele, some aspects of SBMA appear to be driven by a toxic AR independent of androgens whereas others by native androgen-dependent AR function. Values plotted are group means (*N* for motor function and *n* = synaptic function) ± SEM. Myogenic group: WT + B: $n/N = 41/4$ and WT + T: $n/N = 29/3$; Tg + B: $n/N = 30/3$ and Tg + T: $n/N = 40/4$. AR97Q group: WT + B: $n/N = 29/3$ and WT + T: $n/N = 30/3$; Tg + B: $n/N = 41/4$ and Tg + T: $n/N = 40/4$. *n* is the number of endplates per experimental group and *N* is the number of mice per experimental group. $^{*}P < 0.05$ from WT + B or WT + T; $^{\#}P < 0.05$ from Tg + B. 'B' denotes Blank -treated; 'T' Testosterone-treated.

fiber function (e.g. RMP) is comparably perturbed in *both* models, then evidence from the myogenic model would indicate that AR acts in a cell autonomous fashion to trigger the dysfunction. Likewise, if pre-synaptic function (e.g. QC) is comparably disrupted in both models, then data from the myogenic model indicates that muscle AR acts in a *non*-cell autonomous fashion to disrupt pre-synaptic function. Such information is critical for identifying the appropriate cellular target for therapeutics.

T treatment triggered a robust disruption of motor function in asymptomatic Tg females (Fig. 5A), although myogenic females reached end-stage sooner (within 5 days) than AR97Q females (by 2 weeks). End-stage was defined as <30 s hang time. Likewise, androgen also induced synaptic dysfunction (Fig. 5B–I) comparable with that of chronically impaired gonadally intact Tg males, offering additional confirmation of the androgen-dependent and proximate nature of these deficits. Like chronically diseased AR97Q males, the RMP of fibers from T-treated symptomatic myogenic and AR97Q females was significantly depolarized compared with T-treated WT controls (Fig. 5B, Tg + T versus WT + T: $P < 0.001$), with residual deficits in RMP for blank-treated asymptomatic Tg females comparable with asymptomatic castrated AR97Q males (Fig. 5B, Tg + B versus WT + B: $P < 0.001$). This defect in RMP in asymptomatic AR97Q likely depends on expression of a disease-causing AR allele that is independent of androgen exposure, as WT females exposed to androgens do not exhibit a comparable defect in RMP (23).

Androgen-treated *symptomatic* AR97Q females also exhibited significantly increased mEPP amplitude compared with asymptomatic Tg and WT controls (Fig. 5C, Tg + T versus Tg + B or versus WT + T: $Ps < 0.001$), paralleling the effects found for pre-symptomatic and chronically diseased AR97Q Tg males. Such an effect on mEPP amplitude was not seen in symptomatic myogenic females (Fig. 5C, Tg + T versus Tg + B or versus WT + T: $Ps > 0.05$). On the other hand, EPP amplitude was significantly reduced in diseased myogenic females (Fig. 5D, Tg + T versus Tg + B or versus WT + T: $Ps < 0.05$) but not in diseased AR97Q females (Fig. 5D). Thus, acutely diseased Tg females from both models showed significant losses in QC, with fewer but larger quanta in diseased AR97Q females but only fewer quanta in diseased myogenic females (Fig. 5E, Tg + T versus Tg + B or versus WT + T: $P < 0.05$ for myogenic and $P < 0.01$ for AR97Q). Control asymptomatic Tg females from each model also showed reductions in QC, reaching significance in AR97Q females (Fig. 5E, Tg + B versus WT + B: $P < 0.05$). These data are consistent with the idea that reduced evoked transmitter release, like depolarized RMP, are early mechanisms of disease that occur prior to overt motor symptoms independent of androgen. That we find comparable defects in QC and RMP in asymptomatic myogenic females as in asymptomatic AR97Q females suggest that AR acts in a cell autonomous fashion in muscle fibers to disrupt RMP and QC. Androgen treatment also significantly reduced mEPP frequency for both Tg and WT females of both models (Fig. 5F), indicating that androgens can regulate the rate of spontaneous release of neurotransmitter from nerve terminals of the EDL muscle in mice independent of disease.

Both mEPP and EPP decay times were significantly prolonged in diseased AR97Q females (Fig. 5G–I, Tg + T versus Tg + B or versus WT + T: $P < 0.001$ and $P = 0.06$, respectively), whereas only EPP decay time was significantly prolonged for diseased myogenic females (Fig. 5G–I, Tg + T versus Tg + B: $P = 0.003$). Testosterone also prolonged EPP decay time in WT controls, but less than for diseased females and only in the AR97Q model (Fig. 5G). Because both models are on the same C57 of mouse strain background, the significance of this effect in the AR97Q model is not clear, particularly because decay times are not prolonged in gonadally intact WT males compared with castrates in this model.

To further probe the underlying molecular changes and their androgen dependence in disease, we examined the expression of the same genes in muscles of acutely diseased AR97Q and myogenic females. As expected, T treatment of females not only triggered synaptic and motor dysfunction, but also comparable pathological changes in muscle gene expression as seen in chronically diseased males (17,7) (Fig. 6A–D). The adult isoform AChR ϵ-subunit was significantly reduced in both diseased myogenic (Tg + T versus Tg + B or versus WT + T: $P = 0.009$ and $P = 0.002$, respectively, Fig. 6A) and AR97Q females (Tg + T versus Tg + B or versus WT + T: $P = 0.02$ and $P = 0.008$, Fig. 6B) with a complementary increase in mRNA for the neonatal isoform AChR γ-subunit but only for diseased AR97Q females (Tg + T versus WT + T: $P = 0.0035$, Fig. 6B). These data are consistent with the notably prolonged mEPP decay for synapses in AR97Q but not myogenic females (Fig. 5I). Adult Nav1.4 mRNA was also significantly decreased, but only in the myogenic model (Tg + T versus Tg + B or versus WT + T: $P < 0.001$, Fig. 6A). Interestingly, both acute disease models showed significant increases in the neonatal isoform Nav1.5, with a 4-fold increase for diseased myogenic females and a 7-fold increase for AR97Q females (Fig. 6A and B, Tg + T versus Tg + B or versus WT + T: $P < 0.001$ for myogenic, Tg + T versus WT + T: $P < 0.001$ for AR97Q). The greater increase in Nav1.5 in AR97Q diseased females correlates with the reduced sensitivity to μ-CTX observed only for muscles from T-treated AR97Q females and not T-treated myogenic females. Apparently, a threshold amount of Nav1.5 must be incorporated into the membrane before the sensitivity to μ-CTX is reduced. The rapid time course of disease in myogenic females, requiring only 5 days of androgen exposure for females to become fully symptomatic, likely means that fewer sodium channels were converted in this model compared with AR97Q females where motor symptoms develop over weeks rather than days. Nonetheless, because motor function was severely impaired in both models by the end of treatment, pathological changes in sodium channel gene expression does not appear to underlie the loss of motor function (Fig. 2A). We also found pathological changes in muscle gene expression in asymptomatic Tg females, telling a story similar to that of pre-symptomatic AR97Q Tg males. Expression of adult AChR-ϵ subunit was significantly reduced in asymptomatic females of both models (Fig. 6A, $P = 0.021$ for myogenic) although only marginally in asymptomatic AR97Q females (Fig. 6B, $P = 0.065$) compared with control (WT + B) WT females. These findings parallel our findings in pre-symptomatic AR97Q males, as well as those from chronically diseased males (17). Increases in expression of neonatal isoforms AChR-γ subunit and Nav1.5 also occurred in muscles of asymptomatic females but again only in the AR97Q model (Fig. 6B, Tg + B versus WT + B: $Ps < 0.001$), paralleling symptoms of disease in chronically diseased AR97Q males (17).

The decreased RMP of muscle fibers in diseased females was associated with a down-regulation of Kir2.1 transcripts in both myogenic (Fig. 6C, Tg + T versus Tg + B: $P = 0.018$ or versus WT + T: $P = 0.006$) and AR97Q (Fig. 6D, Tg + T versus Tg + B: $P = 0.03$ or versus WT + T: $P = 0.004$) models. Also as predicted by the electrophysiological results, Kir2.1 transcripts in muscles from asymptomatic Tg females of both models were significantly down-regulated (myogenic: Tg + B versus WT + B: $P = 0.023$; AR97Q: Tg + B versus WT + B: $P = 0.0005$). Although Kir2.2 expression was not affected in T-treated myogenic

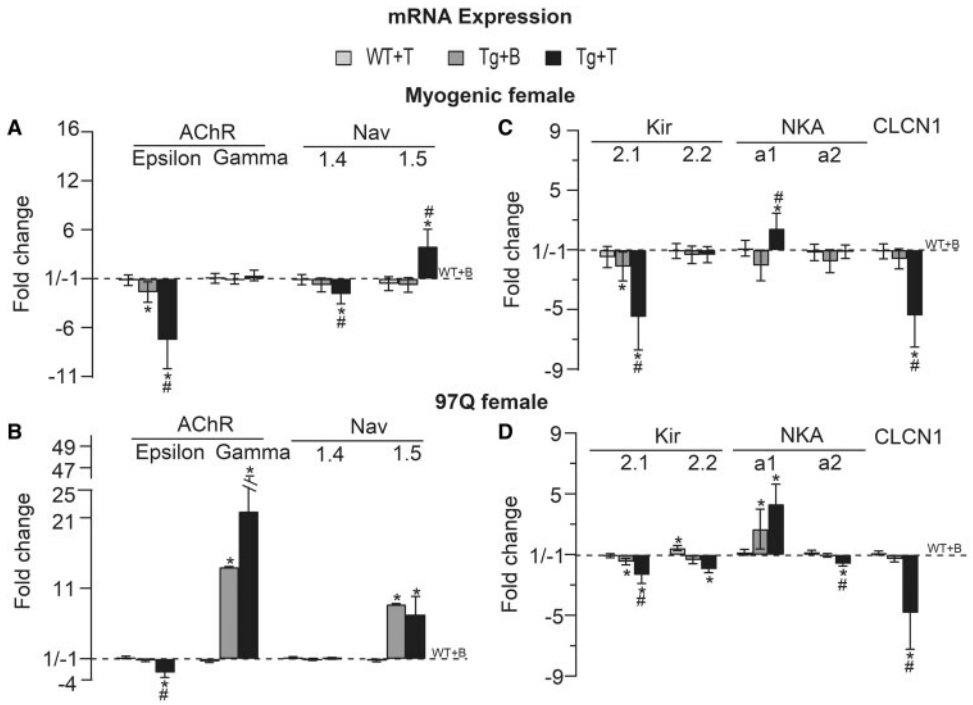

Figure 6. Muscle from acutely diseased females show comparable pathological changes in mRNA expression as chronically diseased males. (**A** and **B**) Acute disease in both models is associated with a significant reduction in the amount of mRNA for the adult isoform AChR ϵ-subunit. A complementary increased expression of the neonatal isoform AChR γ-subunit occurred only in AR97Q females with 2 weeks of treatment, but not in myogenic females, aligning well with prolonged mEPP decay times in diseased AR97Q females but not in diseased myogenic females (Fig. 5I). AChR ϵ-subunit is also reduced in asymptomatic control females of both models, like for pre-symptomatic AR97Q males (Fig. 3). Because controls females are not exposed to exogenous androgens, the milder but nonetheless significant effects on AChR ϵ-subunit suggest that the mutant AR may drive pathological expression of some genes in SBMA muscle independent of androgens, with androgens further exacerbating AR's toxic effects. Only diseased myogenic females show reduced expression of the adult isoform Nav1.4 of the voltage-dependent sodium channel, whereas expression of the immature isoform Nav1.5 is increased significantly by disease in both models. Such changes in mRNA expression for the sodium channel and AChR also occur in chronically diseased males (Fig. 2) (17). These data suggest that the sodium channel and AChR are each early targets of disease. (**C and D**) As expected, mRNA expression of the inward rectifying potassium channel (Kir), the Cl^- ion channel and the NKA pump were affected in both acute models, comparable with chronically diseased males (Fig. 2), and likely underlying the reduced RMP of muscle fibers in each model. Note that Kir2.1 mRNA is significantly down-regulated in both symptomatic and asymptomatic Tg females of both models, but that the magnitude of the change is smaller in asymptomatic control Tg females. These changes correlate well with the magnitude of change in the RMP for symptomatic and asymptomatic myogenic females (Fig. 5B), arguing that changes in Kir2.1 heavily influence the RMP. Kir2.2 is also significantly reduced in acutely diseased AR97Q females and thus, may also contribute to the lowered RMP in this model. Expression of the neonatal isoform of the sodium/potassium pump NKA α1 is up-regulated by disease in both acute models, whereas the adult NKA α2 isoform is significantly reduced only in acutely diseased AR97Q females. *Clcn1* mRNA expression is significantly reduced in both acute models, paralleling the effects of disease on *Clcn1* expression in chronically diseased males (Fig. 2). These data provide further evidence that disease affects specific aspects of synaptic and muscle function, and that these disease events occur early but with a distinct time line of progression, with some representing pre-clinical aspects of the disease. Values are mean fold changes ± SEMs normalized to control WTs (WT + B) based on N/group. Myogenic group: WT + B, WT + T, Tg + B and Tg + T: $N = 6$. AR97Q group: WT + B and WT + T: $N = 5$; Tg + B and Tg + T: $N = 4$. $^*P < 0.05$ from WT + B or WT + T; $^\#P < 0.05$ from Tg + B. 'B' denotes Blank -treated; 'T' Testosterone-treated.

females, it was significantly down-regulated in T-treated AR97Q females (Fig. 6D, Tg + T versus Tg + B: $P = 0.2$ or versus WT + T: $P = 0.008$), again paralleling changes observed in chronically diseased males of both models (Fig. 2B and unpublished observation). NKA α1 expression level was also significantly up-regulated in diseased muscle from both female models (Fig. 6C and D, Tg + T versus Tg + B: $P = 0.002$ or versus WT + T: $P = 0.032$ for myogenic, Tg + T versus WT + T: $P = 0.001$ for AR97Q), as well as in muscles from asymptomatic AR97Q females (Tg + B versus WT + B: $P = 0.016$), albeit smaller in magnitude. Androgen also induced a down-regulation in the adult NKA α2 isoform but only for AR97Q females (Tg + T versus Tg + B: $P = 0.03$ or versus WT + T: $P = 0.0015$). These changes in acutely diseased females are comparable with those of chronically diseased males in both AR97Q and myogenic models (Fig. 2B and unpublished observation). *Clcn1* mRNA level was also reduced in both myogenic (Tg + T versus Tg + B or versus WT + T: $P = 0.0035$ and $P = 0.005$, respectively) and AR97Q females (Tg + T versus Tg + B or versus WT + T: $P = 0.026$ and $P = 0.002$, respectively) (Fig. 6C and D), comparable with that of diseased males in both models (7). These data raise the possibility that muscle ion channels and ion transporters are perturbed pre-clinically independent of androgens, with androgens further driving such pathology to result in the overt loss of muscle strength and endurance.

Discussion

Previous work indicates multiple core deficits in neuromuscular transmission and muscle function that may underlie motor dysfunction in SBMA mice (17,24). In this study, we asked if such deficits are androgen-dependent, a key distinguishing feature of SBMA, and if such deficits are expressed prior to overt losses in motor performance. To answer these questions, we recorded intracellularly from muscle fibers of castrated AR97Q males with rescued motor function and from muscle fibers of androgen-treated, acutely diseased Tg females of two different models, AR97Q and myogenic. We also examined synaptic and muscle function in *pre*-symptomatic AR97Q

males. Quantitative PCR was used to track mRNA expression for several key proteins controlling synaptic and muscle function. Our main findings are: (1) Defects in neuromuscular transmission and muscle function are androgen-dependent and correlate well with motor dysfunction. (2) Castration largely rescues synaptic strength (based on QC) and membrane excitability of muscle fibers (based on the RMP) in AR97Q males, correlating with rescued motor function. However, significant residual deficits in both measures persist despite the lack of gonadal androgens, raising the question of whether some aspects of AR toxicity are independent of androgens. (3) Notably, these same defects in QC and RMP occur early, before motor dysfunction, in AR97Q males, suggesting that both are pre-clinical symptoms of disease. (4) Tg females show a similar pattern, with small but significant defects in QC and RMP in asymptomatic females, which are increased in magnitude by androgens as robust motor dysfunction is induced. (5) Such changes in synaptic and muscle function tightly correlate with changes in mRNA expression of key genes controlling these functions, namely ligand- or voltage-dependent ion channels (the AChR and channels for sodium, potassium, and chloride) and ion transporters (the sodium/potassium pump). Our findings implicate several novel biomarkers in muscle that underlie pre-clinical and clinical symptoms of SBMA (Tables 1 and 2). Together, these findings indicate that specific cellular defects precede overt phenotypic characteristics of motor dysfunction. Postsynaptic ion channels and ion transport mechanisms that control the resting voltage, and hence the excitability of muscle fibers, are early molecular targets of AR toxicity, as are presynaptic mechanisms controlling the probability of neurotransmitter release. It appears that the progressive, androgen-driven loss of motor function involves the cumulative effects of these and other androgen-dependent defects that develop over time. Whether preventing early defects in QC and RMP will prevent other functional defects from developing and preserve motor function is the next critical question to answer in an effort to find druggable targets that could potentially protect or rescue motor function in SBMA patients independent of endogenous androgens.

Early events of disease and their androgen dependence

Pre-pubertal castration of pre-symptomatic AR97Q males fully protected their motor function, as previously shown (10). Along with that, defects in muscle RMP and presynaptic release of QC were largely, but not fully prevented in these same castrated AR97Q males. We were surprised that muscles from pre-pubertal asymptomatic AR97Q males also exhibited defects in RMP and QC, which were comparable with that of chronically diseased end-stage AR97Q males, despite the fact that pre-symptomatic mice exhibit good motor function. These findings have two important implications: (1) Significant defects in RMP and QC emerge early, and may underlie pre-clinical symptoms of SBMA that typically involve aberrant muscle activity (muscle fasciculations and cramping). Such reduced RMP of muscle fibers is associated with hyper-excitability of the fiber membrane (17). Even small spontaneous events may reach threshold for contraction given the increased excitability of muscle fibers. This effect could readily explain the spontaneous muscle contractions that plague SBMA female carriers and pre-clinical symptoms of males who have the CAG expanded *AR* gene. Given that our current measures of motor function are relatively crude and unlikely to capture pre- (or 'sub') clinical symptoms of SBMA, the term 'pre-symptomatic' must be viewed with caution. What is clear, however, is that significant defects in both QC and RMP are not sufficient, but may be necessary, for overt motor dysfunction (typically on the basis of loss of strength and endurance). (2) Although a substantial portion of the defect in QC and RMP is androgen-dependent, another portion of the defect may not be. Supporting the idea that some aspects of the disease process may be independent of androgens are the findings that both asymptomatic AR97Q males castrated peri-pubertally and Tg females have notable defects in QC and RMP. Importantly, asymptomatic Tg females were never exposed to male levels of androgens. These data raise the distinct possibility that some toxic actions of a mutant AR may occur independent of androgens, setting the stage of development of clinical symptoms of disease. On the other hand, androgen exposure begins prenatally in males, and androgen action during development has lasting and irreversible effects on cell morphology and function (25). Thus, androgens acting on a mutant AR before puberty may have triggered defects in QC and RMP that are not reversible by removing androgens later on. Also note that the magnitude of the defects in both QC and RMP in pre-pubertal pre-symptomatic males is comparable with that of chronically diseased adults, suggesting that most of the adult defect in QC and RMP develops before puberty. Because a large portion of this deficit was reversed by removing androgens at the onset of puberty, the possibility remains that defects in QC and RMP depend fully on androgens, with some before and some after puberty. Depriving AR97Q males of their own androgens earlier in development would shed light on this issue. It is also possible that Tg females are exposed to sufficient amounts of androgens (from the ovaries and adrenals) over the long run to induce pre-clinical symptoms. Notably, Tg AR97Q females eventually develop severe motor defects comparable with Tg males but with an appreciably delayed time course (10). However, further questioning the role of androgens in SBMA are two unexpected findings: (1) castration does not rescue motor function in mid to late stage symptomatic AR97Q males (unpublished observation) and (2) androgen reduction therapy given pre-clinically to an XY individual with an expanded (49 CAG repeat) AR failed to prevent the emergence of clinical symptoms (e.g. muscle weakness and fatigue, cramps, throat spasms, difficulty climbing stairs) of SBMA (19,26). Moreover, the inability of castration to rescue function in fully symptomatic AR97Q males is not explained by a loss of motoneurons, because there is little to no evidence that motoneurons die in this model (10). In summary, there may be aspects of the disease that are genuinely independent of androgens, but nonetheless driven by a toxic AR. Recent clinical observations are also consistent with the idea that although androgens seem to have a role, it is not clear to what extent and when their action might trigger an irreversible path toward disease (26).

Pre-clinical markers of SBMA and putative mechanisms involved

Defects in synaptic facilitation and QC characteristic of end-stage AR97Q males are products of defects in two distinct *presynaptic* mechanisms: reduced size of the RRP and low probability of transmitter release (17). Notably, synaptic facilitation and QC are also affected in pre-symptomatic males. Further analysis of neurotransmission in pre-symptomatic males revealed that only Pr, not RRP size, was affected. From these data, it seems likely that mechanisms controlling Pr are affected first in SBMA and likely before overt muscle weakness is experienced by the patient, followed by later effects on the size of the RRP that

further weaken neuromuscular synapses by reducing QC even more. This loss in synaptic drive likely contributes to the patient's initial symptoms of muscle weakness and fatigue.

The molecular mechanisms, and thus potential druggable targets, for controlling Pr are many. The RRP and Pr are in some ways intimately connected. Factors that affect the size of the RRP, like the SNARE complex that renders synaptic vesicles anchored and fusion-competent, will necessarily affect Pr (27). On the other hand, changes in Pr do not necessarily affect the size of the RRP. Given that pre-symptomatic AR97Q males show only a deficit in Pr, there are fewer potential candidates that mutant ARs might have perturbed. One likely possibility is that the distribution and abundance of voltage-gated calcium channels in the active zone has been altered, factors known to profoundly influence Pr. Our findings from a knockin (KI) mouse model of SBMA indicate that all three forms of transmitter release (synchronous, asynchronous and spontaneous) are reduced in early-stage KI mice, strongly suggesting that disease affects this population of calcium channels, implicating effects on scaffolding proteins that form the cytomatrix. Candidate molecules in the cytomatrix include the activity-regulated RIM, its binding proteins, and liprin-α. The amount of RIM in the nerve terminal can directly control the number of calcium channels in the active zone and thus, Pr. The calcium channel auxiliary subunit ($\alpha_2\delta$) that mediates protein–protein interactions, particularly between the extracellular matrix and cell adhesion proteins, also contributes to the distribution and number of calcium channels in the presynaptic plasma membrane, and thus Pr (28). Other potential candidates could directly modulate calcium flux via their channels. One such protein is Munc13, shown to regulate the kinetic properties of voltage-gated calcium channels in the presynaptic nerve terminal (29). A particularly intriguing candidate is brain-derived neurotrophic factor (BDNF), which can regulate the developmental switch from the immature state of a mix of N- and P/Q-type calcium channels to exclusively P/Q-type channels in an activity-dependent manner (30), two channels with distinct functional properties that affect Pr. Because BDNF expression is also perturbed in diseased SBMA muscle (31), and AR can act in muscle to impair pre-synaptic Pr, BDNF is a particularly attractive potential therapeutic to explore. Muscle-derived neurotrophic factors in general offer a model for understanding how disease originating in muscle impairs function in the motoneurons (17).

The other main pre-clinical symptom we discovered was a ∼20 mV depolarizing shift in the RMP of muscle fibers. When the RMP sits closer to threshold, it causes fibers to be hyperexcitable (17). Mechanisms behind this shift in the RMP seem clear, appearing to be caused by switches in the isoforms for the potassium channel and sodium/potassium pump, the main two molecular players controlling the RMP. In muscles from affected adult AR97Q males, message encoding the α1 subunit of the Na^+, K^+ (NKA) pump is significantly upregulated (∼4-fold) compared with that of age-matched WTs, whereas levels of α2 mRNA show a 1.5-fold deficit. Pre-pubertal castration restores both to near but not completely to WT levels, aligning well with effects on the RMP, which was also nearly, but not completely, restored to WT levels. On the other hand, message for the two subunit isoforms of the potassium channel Kir2.1 and 2.2 were significantly reduced by disease and fully restored to normal by pre-pubertal castration of AR97Q adult males. Notably, these same molecular players are perturbed in muscles from pre-symptomatic AR97Q males, paralleling a comparable depolarizing shift in the RMP. Because muscles from pre-symptomatic AR97Q males show significant deficits in mRNA for Kir2.1 and NKA α2 without deficits in the other subunit isoforms, they are likely the proximate molecular players underlying the enhanced excitability of SBMA muscle fibers. Potassium channel Kir2.1 was also downregulated in acutely diseased myogenic and AR97Q females, although only AR97Q females with 2 weeks of androgen exposure showed an effect of disease on expression of sodium/potassium NKA α2. These data implicate the inward rectifier potassium channel as a potent regulator of fiber RMP and as a particularly early target of disease. Although mRNA for the chloride channel also shows marked deficits in muscle of pre-symptomatic AR97Q males, we find little evidence that chloride conductance contributes significantly to the RMP of mouse skeletal muscle fibers (-69.9 ± 1.1 and -69.6 ± 0.9 mV before and after perfusing with Cl^{-1}-free solution from 40 muscle fibers of WT males). Overall, our results show that deficits in QC and muscle fiber RMP are two pre-clinical markers of disease that may set the stage for further demise and implicate specific molecules as therapeutic targets for treating pre-clinical symptoms of SBMA and possibly preventing disease progression.

It is also worth pointing out that some disease correlates of synaptic and muscle dysfunction in chronically diseased AR97Q males are not present pre-symptomatically in AR97Q males, nor in acutely diseased adult myogenic females. For example, synapses of pre-symptomatic AR97Q Tg males and acutely diseased myogenic females do not show the slowed decay times in mEPPs characteristic of chronically diseased synapses. Predictably, neither express the immature mRNA isoform of the AChR, the gamma subunit. Likewise, muscles from pre-symptomatic AR97Q males also do not show a reduced sensitivity to μ-CTX nor the upregulated expression of the immature isoform of the sodium channel characteristic of chronically diseased AR97Q adult males. These data underscore the fact that as the disease progresses, so does the underlying cell and synaptic pathology, along with an expanding network of dysregulated genes that control these functions. However, it is yet to be determined whether rescuing early pathogenic outcomes such as neurotransmitter release and fiber RMP would halt the sequence of pathological events that would ordinarily follow to drive disease progression.

Amplification of normal AR action may underlie some aspects of disease

In the androgen-sensitive levator ani muscle, androgens normally inhibit spontaneous transmitter release without affecting evoked release (23,32,33). Interestingly, we find that T treatment similarly reduces the frequency of spontaneous release in the EDL muscle of both WT and Tg females of both models without affecting evoked release in WT females (Fig. 5). Not only do these data indicate that androgens normally affect spontaneous and evoked release differently, but they also raise the possibility that some apparently toxic effects of a mutant AR may reflect the amplification of normal AR action, an idea previously posed (34). Note that although mEPP frequency is unaffected in chronically diseased synapses of adult AR97Q males, it is reduced in pre-symptomatic AR97Q males, just as it is in KI SBMA males (17), implicating changes in mEPP frequency as possibly a very early event in the disease process leading to deficits in evoked quantal release (QC). Androgens apparently exert their inhibitory influence on spontaneous release by regulating a mechanism yet to be identified that links presynaptic calcium channels to the transmitter release machinery (33). Protecting this mechanism from the deleterious effects of androgens in SBMA may offer a way to protect quantal release, which in turn may prevent muscle fibers from compensating to increase their

excitability by reducing their RMP (35,36). An important next step is to identify this potentially pivotal early mechanism that may trigger further pathogenesis.

Innovative therapeutic approaches for treating SBMA

Our data have clear implication for new approaches to therapeutics. For example, the depolarized state of muscle fibers might trigger the progression of disease in SBMA. Because Kir channels and the NKA pump are primary mechanisms for regulating the RMP of muscle fibers, drugs that regulate these two mechanisms may be effective therapeutics for SBMA. Although drugs directly targeting Kir or NKA pump are not yet available, drugs called potassium channel openers (KCOs) target two different potassium channels, big Ca^{2+} activated K^+ channels (BK_{Ca}) and ATP-sensitive K channels (K_{ATP}) (37,38), that effectively restore the normal RMP of skeletal muscle fibers in both humans and animals as a treatment for paralysis or myotonia (39–42). Our data also suggest that strategies to improve neuromuscular transmission may also be effective therapeutics. We find considerable evidence for neurotransmission failure in pre-symptomatic AR97Q males, which shows that most nerve-evoked synaptic potentials fail to elicit action potentials in the muscle fiber, whereas direct stimulation of the muscle reliably evokes action potentials (unpublished observation). These data indicate that neurotransmission failure caused by impaired transmitter release is a predominate feature of neuromuscular synapses pre-symptomatically. Neurotransmission failure could explain why muscle fibers in SBMA mouse models exhibit a denervation-like phenotype even though the fibers are innervated (15,17). To increase synaptic strength, 3,4-diaminopyridine phosphate (3,4-DAP, amifampridine), a delayed-rectifier K channel blocker, a leading treatment for Lambert–Eaton myasthenic syndrome (LEMS) (43) may have therapeutic value for SBMA patients. LEMS is an autoimmune disorder with impaired neuromuscular transmission caused by insufficient synaptic release of acetylcholine (44). 3,4-DAP blocks both fast and slow potassium channels in motor nerve terminals and prolongs the depolarization phase of the nerve action potential, thereby increasing the open-time of voltage-gated calcium channels, ultimately enhancing the amount of ACh released by the nerve terminal. 3,4-DAP has also been found to benefit patients with congenital myasthenic syndromes (43), and improve muscle force in normal and fatigued muscle independent of disease (45). That all three forms of transmitter release (synchronous, asynchronous and spontaneous releases) are reduced along with reduced probability of release in diseased Tg mice indicates that calcium channels are a likely target of AR toxicity. Thus, 3,4-DAP might be a beneficial treatment for SBMA. Finally, acetylcholinesterase (AChE) inhibitors, a main treatment for myasthenia gravis, improve neuromuscular transmission by increasing the half-life of acetylcholine. The AChE inhibitor pyridostigmine has been reported to increase stamina in SMA patients (46), further suggesting that it may also be beneficial in treating SBMA. Significantly, our data point to a number of already FDA-approved drugs that could potentially help SBMA patients now.

Materials and Methods

SBMA mouse models

All experiments were done in accordance with NIH guidelines and approved by the Institutional Animal Care and Use Committee.

AR97Q model

Tg mice were generated with ubiquitously expressing cDNA encoding a full length human AR with AR97Q repeats under the control of a CMV enhancer/chicken β-actin promoter (10) and maintained on a C57Bl/6J in our breeding colony at Michigan State University. Tg males develop motor symptoms during early adulthood.

Castrated AR97Q male

Pre-pubertal Tg and WT males were castrated (Tg + C, WT + C) or sham operated (Tg + S, WT + S) via the abdominal route under isoflurane anesthesia at postnatal days 30–32. Behavior was monitored twice weekly starting on the day prior to surgery until sham operated (Tg + S) males reached end-stage (hang time < 30 s), at which point it and its age-matched controls (Tg + C, WT + C and WT + S) were used for study. The age range of study was 63–95 postnatal days for electrophysiology recording. Muscles for gene expression analyses using RT-qPCR were harvested from a separate cohort of age-matches males (aged 55–104 postnatal days).

Pre-symptomatic AR97Q male

Muscle was dissected from pre-symptomatic AR97Q ranging in age from 33 to 40 postnatal days. Behavior was monitored up to day before dissection. Muscles for gene expression analyses using RT-qPCR were harvested from a separate cohort of pre-symptomatic AR97Q mice and aged-matched WT controls aged 29–32 postnatal days. Behavior was not monitored for this cohort.

Acutely diseased AR97Q female

Tg and age-matched WT female mice ages 50–78 days old were implanted subcutaneously with Silastic capsules containing either crystalline free T or nothing (Blank-treated) under isoflurane anesthesia (the effective release length of capsule: 6 mm, inner diameter: 1 mm, outer diameter: 3 mm; soaked in sterile phosphate-buffered saline overnight). Behavior was monitored twice weekly starting on the day prior to surgery and muscle was dissected and examined when T-treated Tg female reached end-stage (hang time < 30 s, about 14–17 days after T-treatment). Muscles for gene expression analyses using RT-qPCR were harvested from a separate cohort of age-matched females (aged 64–73 postnatal days).

Myogenic model

Tg mice overexpressing the rat WT AR exclusively in skeletal muscle fibers were described previously (5). In brief, Tg mice were generated using the human skeletal α-actin promoter to drive expression of a rat AR transgene specifically in skeletal muscle fibers. Tg mice and age-matched WT controls used for the current study were maintained on a C57BI/6J background from the symptomatic 141 line, that were exposed prenatally to flutamide to block the effects of prenatal endogenous androgens to enhance neonatal survival of Tg males (47). Inclusion of this model allows us to specifically evaluate the role of muscle AR on neuromuscular function. If results from this model parallel the results found in the AR97Q model in which mutant AR is globally expressed, these data provide compelling evidence that the effect of disease on given outcomes measures is mediated via muscle AR. This information delineates where therapeutics should be directed.

Acutely diseased myogenic female

The survival of Tg females does not depend on prenatal flutamide as it does for Tg males but the females used in our studies

were from litters exposed to flutamide prenatally. Two separate cohorts of mice were studied for the electrophysiology analysis (age-matched Tg and WT female mice 80–255 days of age) RT-qPCR analysis (101–153 days of age). Myogenic females were implanted subcutaneously with Silastic capsules as described earlier for AR97Q females. Their motor function was assessed immediately prior to surgery and daily thereafter during the five days of treatment. On day 5, the EDL was dissected for study.

Motor function tests

Limb muscle strength was evaluated using the hang test. The hang test was conducted by placing mice on a cage lid that was then turned upside-down 40 cm above a counter. Latency to fall up to 120 s was measured (5). Mice with less than maximal time on the first test were tested up to two more times, and the highest recorded hang time in that session/day was used for that mouse. Data were collected blind to genotype and treatment condition.

Electrophysiology

Solutions

The external physiological solution used for the dissection and recording had the following compositions (in mM): 135 NaCl, 5 KCl, 2 $CaCl_2$, 1 $MgCl_2$, 14 HEPES, 11 D-glucose, pH adjusted to 7.4 by NaOH.

Neuromuscular preparation

Mice were deeply anesthetized with carbon dioxide inhalation and sacrificed by decapitation. EDL muscle and its attached nerve were dissected under oxygenated physiological solution and pinned at approximate resting length in a small Sylgard-coated chamber.

Intracellular recording

The pinned neuromuscular preparation was perfused continuously at a rate of 1–5 ml/min with fresh oxygenated Ringer's at room temperature (23–25°C). Preparations were equilibrated for at least 20–30 min to ensure its stability before data acquisition began. μ-CTX GIIIB (Alomone Labs), which blocks voltage-gated sodium channels in muscle was used to block muscle contraction during nerve stimulation. Neuromuscular preparations from WT mice were incubated for 15–20 min in Ringer's containing 2.5 μM μ-CTX and Tg mice incubated for 20–60 min in Ringer's containing 5 μM μ-CTX. Tg muscle required more and longer incubations in μ-CTX than WT muscle because of the aberrant expression of neonatal sodium channels in Tg muscle (17). Preparations were re-exposed to μ-CTX after 1–2 h to maintain contraction block. EPPs and spontaneous mEPPs and RMP were recorded as described previously (17). The RMP was used to correct for differences in driving force and non-linear summation of EPPs (48,49). The nerve was stimulated with square-wave pulses of 0.05–0.5 ms duration at 0.5 Hz, with suprathreshold voltage, by means of a suction electrode attached to a stimulus isolation unit (Grass SIU, Grass Instruments, Quincy, MA) and stimulator (Grass S48). Signals were amplified using an Axoclamp-2B amplifier (Molecular Devices, Sunnyvale, CA), acquired with Clampex version 10.3 using an analog-to-digital converter (DigiData 1440A, Molecular Devices, Sunnyvale, CA). Synaptic facilitation was evaluated using trains at 0.5 Hz of five pulses at 100 Hz (10 ms interpulse interval within the train). Tetanizing stimulation was delivered at 100 Hz for 0.5 s to evaluate the size of the RRP and Pr (50). The minimum interval between tetanizing stimulus trains was 5–10 min that was sufficient for full recovery of EPP amplitude. Genotype and treatment condition were known by experimenter.

Data analysis

Off-line analysis was performed using Clampfit version 10.3. To minimize the possible contribution of differences in RMP, and thus differences in the driving force across preparations on synaptic potential amplitudes, EPP and mEPP amplitudes were normalized to a consistent theoretical resting level of –75 mV, assuming that 0 mV is the equilibrium potential for ACh-induced current under the present recording conditions. The relationship: $EPP' = EPP_{normalized}/[1 - f(EPP_{normalized}/E)]$ was subsequently used to correct for nonlinear summation. E is the difference between the membrane potential (V_m) and the equilibrium potential for ACh current (0 mV). The value f (set to 0.8) is a factor that improves the accuracy of the nonlinear correction by taking into account the effect of the membrane capacitance of the muscle fiber. The QC (the number of ACh quanta released per nerve impulse) at each NMJ was calculated by using the ratio of the EPP′ and the normalized mEPP amplitude. mEPPs recorded for a period of 2–5 min were analyzed by using the template search algorithm in Clampfit 10.3 The template was constructed by averaging 5–10 mEPPs. All mEPPs identified by the program were inspected and the Template Match Threshold Parameter was adjusted to minimize false positives. The rise time (10–90%) and decay time (90–10%) of EPPs and mEPPs were also measured. Cumulative histogram distributions were used to compare the amplitude of mEPPs between diseased and WT.

The size of the RRP in pre-symptomatic AR97Q males was evaluated during 50 stimuli in response to 100 stimulation and obtained by plotting QC against cumulative number of quanta and back-extrapolated from the linear portion of the curve to the x-axis intercept (Fig. 4C). The x-intercept gave an estimate of the size of the RRP. The probability of release was estimated by dividing the QC of the first EPP by RRP size (50–53). Data were exported from Clampfit and plotted by using Igor software (Wave metrics, Lake Oswigo, OR).

Recordings from each end-plate or muscle fiber are reported as mean values ± standard error of the mean (SEM) with n being the number of endplates per experimental group and N the number of mice per experimental group. All reported results are on the basis of at least three to four animals per genotype within each model. Statistical analysis of data for castrated male and T-treated female groups was performed using two-way analysis of variance with genotype (Tg or WT) or hormone treatment (sham versus castrate in males; T versus blank in females) as independent variables and Bonferroni t-test was used to determine significant differences for planned pairwise comparisons (Sigmaplot, Systat Software Inc., San Jose, CA). For pre-symptomatic AR97Q male group, statistical comparisons were made comparing data from diseased mice to their own WT littermates using Student's unpaired t-test. Kolmogorov–Smirnov (K-S) test was used to compare the significance of the distribution of mEPP amplitudes. Results were considered statistically significant when the P value was <0.05.

Gene expression analysis

We examined gene expression via RT-qPCR in EDL muscle for sham and castrated adult AR97Q males and T or blank-treated

Table 3. Target genes and their respective primers used for examining gene expression in castrated AR97Q EDL and pre-symptomatic AR97Q TA muscles

Transcript	Forward primer	Reverse primer
Rn18s	GGACCAGAGCGAAAGCATTTG	GCCAGTCGGCATCGTTTATG
Chrne	CTCTGCCAGAACCTGGGTG	TGTGCTCTCAGCCACAAAGT
Chrng	GGTTGGTGATGGGTATGGTCA	TGACATCAGGAAAGGCAGAGC
Scn4a	TGGGGGTCAACTTGTTTGCT	TCGAATCTCTCGGAGGTGGT
Scn5a	GTCTCAGCCTTACGCACCTT	TCCCACGATTGTCTTCAGGC
Clcn1	GATTTGCTGCGGGTTCTTGG	TGGCTGAGACACTTGTGCTT
Kcnj2	AAGCGTACCTCTAGAGCCCA	GACCAACGTCAGGCTGTGTA
Kcnj12	CACCATTGGCTACGGGCTAC	TCAATGATGCAGCCCACAATG
Atp1α1	GAAGCTGACACCACGGAGAA	TAGCCTGAAACACTGCCCTG
Atp1α2	TGGACTGGGATGATCGGACT	ACTGCACAACCACGATGCTA

myogenic and AR97Q females, and in the tibialis anterior (a fast twitch muscle, similar in fiber type composition to the EDL) for pre-symptomatic AR97Q males. These larger muscles provided the requisite RNA yield. Tissue samples were frozen in RNase-free tubes on dry ice, and held at –80°C until processed. Instruments used for dissection were cleaned with RNaseZap (Sigma-Aldrich) between animal harvests.

RNeasy Fibrous Tissue Mini Kit (Qiagen) was used to extract RNA from muscle samples. Tissue was mechanically homogenized with a PRO200 homogenizer (Pro Scientific). Following extraction, RNA was quantified on a spectrophotometer (Beckman DU 530) by measuring 260 nm absorbance values. Extracted RNA was then reverse transcribed using the High Capacity cDNA Reverse Transcription Kit (Applied Biosystems) with the following thermocycle: 25°C for 10 min, 37°C for 2 h and 85°C for 5 min. Each RT-qPCR sample included 2.5 ng of cDNA, primers, and Power SYBR Green PCR Master Mix (Applied Biosystems). Thermocycle for the quantitative step on the ABI PRISM 7000 Sequence Detection System was as follows: 50°C for 2 min, 95°C for 10 min and 40 cycles of 95°C for 15 s and 60°C for 1 min. A dissociation curve was determined for each well to confirm that only one product was amplified. Each sample was run in triplicate. Samples without reverse transcriptase during the cDNA conversion were also assessed to ensure that there was no DNA contamination. Optimal concentrations and amplification efficiencies were calculated for each primer set. The reference gene was 18S. Target genes and primer sequences are listed in Table 3.

Relative Expression Software Tool was used to assess statistical significance and fold change of genes (54). Specifically, this software uses the non-parametric Pair-Wise Fixed Reallocation Randomization Test to account for amplification efficiencies when determining fold change. It measures relative expression of a target gene between a control (WT) and sample (Tg) group following the normalization of the target gene to a reference gene (18S). The criterion for statistical significance was $P < 0.05$. Analysis was done blind to genotype and treatment condition.

Acknowledgements

We thank Diane Redenius and Monika Werbanowska for technical assistance in breeding, genotyping and testing the motor function of mice, Beth Kenyon for processing RNA and running qPCR and Juli Wade for her generosity in allowing us to use her real time machine.

Conflict of Interest statement. None declared.

Funding

National Institutes of Health (R01NS-045195, C.L.J.).

References

1. Sobue, G., Hashizume, Y., Mukai, E., Hirayama, M., Mitsuma, T. and Takahashi, A. (1989) X-linked recessive bulbospinal neuronopathy. A clinicopathological study. *Brain*, **112**, 209–232.
2. La Spada, A.R., Wilson, E.M., Lubahn, D.B., Harding, A.E. and Fischbeck, K.H. (1991) Androgen receptor gene mutations in X-linked spinal and bulbar muscular atrophy. *Nature*, **352**, 77–79.
3. Schmidt, B.J., Greenberg, C.R., Allingham-Hawkins, D.J. and Spriggs, E.L. (2002) Expression of X-linked bulbospinal muscular atrophy (Kennedy disease) in two homozygous women. *Neurology*, **59**, 770–772.
4. Lieberman, A.P., Yu, Z., Murray, S., Peralta, R., Low, A., Guo, S., Yu, X.X., Cortes, C.J., Bennett, C.F., Monia, B.P. *et al.* (2014) Peripheral androgen receptor gene suppression rescues disease in mouse models of spinal and bulbar muscular atrophy. *Cell Rep.*, **7**, 774–784.
5. Monks, D.A., Johansen, J.A., Mo, K., Rao, P., Eagleson, B., Yu, Z., Lieberman, A.P., Breedlove, S.M. and Jordan, C.L. (2007) Overexpression of wild-type androgen receptor in muscle recapitulates polyglutamine disease. *Proc. Natl. Acad. Sci. U. S. A.*, **104**, 18259–18264.
6. Cortes, C.J., Ling, S.C., Guo, L.T., Hung, G., Tsunemi, T., Ly, L., Tokunaga, S., Lopez, E., Sopher, B.L., Bennett, C.F. *et al.* (2014) Muscle expression of mutant androgen receptor accounts for systemic and motor neuron disease phenotypes in spinal and bulbar muscular atrophy. *Neuron*, **82**, 295–307.
7. Oki, K., Halievski, K., Vicente, L., Xu, Y., Zeolla, D., Poort, J., Katsuno, M., Adachi, H., Sobue, G., Wiseman, R.W. *et al.* (2015) Contractile dysfunction in muscle may underlie androgen-dependent motor dysfunction in spinal bulbar muscular atrophy. *J. Appl. Physiol.*, **118**, 941–952.
8. Soraru, G., D'Ascenzo, C., Polo, A., Palmieri, A., Baggio, L., Vergani, L., Gellera, C., Moretto, G., Pegoraro, E. and Angelini, C. (2008) Spinal and bulbar muscular atrophy: skeletal muscle pathology in male patients and heterozygous females. *J. Neurol. Sci.*, **264**, 100–105.
9. Jordan, C.L. and Lieberman, A.P. (2008) Spinal and bulbar muscular atrophy: a motoneuron or muscle disease? *Curr. Opin. Pharmacol.*, **8**, 752–758.
10. Katsuno, M., Adachi, H., Kume, A., Li, M., Nakagomi, Y., Niwa, H., Sang, C., Kobayashi, Y., Doyu, M. and Sobue, G.

(2002) Testosterone reduction prevents phenotypic expression in a transgenic mouse model of spinal and bulbar muscular atrophy. *Neuron*, **35**, 843–854.
11. Sahashi, K., Katsuno, M., Hung, G., Adachi, H., Kondo, N., Nakatsuji, H., Tohnai, G., Iida, M., Bennett, C.F. and Sobue, G. (2015) Silencing neuronal mutant androgen receptor in a mouse model of spinal and bulbar muscular atrophy. *Hum. Mol. Genet.*, **24**, 5985–5994.
12. Adachi, H., Katsuno, M., Minamiyama, M., Waza, M., Sang, C., Nakagomi, Y., Kobayashi, Y., Tanaka, F., Doyu, M., Inukai, A. *et al.* (2005) Widespread nuclear and cytoplasmic accumulation of mutant androgen receptor in SBMA patients. *Brain*, **128**, 659–670.
13. Rocha, M.C., Pousinha, P.A., Correia, A.M., Sebastiao, A.M. and Ribeiro, J.A. (2013) Early changes of neuromuscular transmission in the SOD1(G93A) mice model of ALS start long before motor symptoms onset. *PLoS One*, **8**, e73846–e73811.
14. Kong, L., Wang, X., Choe, D.W., Polley, M., Burnett, B.G., Bosch-Marce, M., Griffin, J.W., Rich, M.M. and Sumner, C.J. (2009) Impaired synaptic vesicle release and immaturity of neuromuscular junctions in spinal muscular atrophy mice. *J. Neurosci.*, **29**, 842–851.
15. Poort, J.E., Rheuben, M.B., Breedlove, S.M. and Jordan, C.L. (2016) Neuromuscular junctions are pathological but not denervated in two mouse models of spinal bulbar muscular atrophy. *Hum. Mol. Genet.*, **25**, 3768–3783.
16. Kemp, M.Q., Poort, J.L., Baqri, R.M., Lieberman, A.P., Breedlove, S.M., Miller, K.E. and Jordan, C.L. (2011) Impaired motoneuronal retrograde transport in two models of SBMA implicates two sites of androgen action. *Hum. Mol. Genet.*, **20**, 4475–4490.
17. Xu, Y., Halievski, K., Henley, C., Atchison, W.D., Katsuno, M., Adachi, H., Sobue, G., Breedlove, S.M. and Jordan, C.L. (2016) Defects in Neuromuscular Transmission May Underlie Motor Dysfunction in Spinal and Bulbar Muscular Atrophy. *J. Neuorsci.*, **36**, 5094–5106.
18. Dudel, J. and Heckmann, M. (2002) Quantal endplate currents from newborn to adult mice and the switch from embryonic to adult channel type. *Neurosci. Lett.*, **326**, 13–16.
19. Jurkat-Rott, K., Fauler, M. and Lehmann-Horn, F. (2006) Ion channels and ion transporters of the transverse tubular system of skeletal muscle. *J. Muscle Res. Cell Motil.*, **27**, 275–290.
20. Orlowski, J. and Lingrel, J.B. (1988) Tissue-specific and developmental regulation of rat Na, K-ATPase catalytic alpha isoform and beta subunit mRNAs. *J. Biol. Chem.*, **263**, 10436–10442.
21. Radzyukevich, T.L., Neumann, J.C., Rindler, T.N., Oshiro, N., Goldhamer, D.J., Lingrel, J.B. and Heiny, J.A. (2013) Tissue-specific role of the Na, K-ATPase alpha2 isozyme in skeletal muscle. *J. Biol. Chem.*, **288**, 1226–1237.
22. Zhao, C., Zhang, J., Li, K., Yang, J., Yu, H., Duan, S., Jiang, K. and Li, X. (2014) beta-Catenin regulates membrane potential in muscle cells by regulating the alpha2 subunit of Na, K-ATPase. *Eur. J. Neurosci.*, **40**, 2216–2224.
23. Souccar, C., Lapa, A.J. and do Valle, J.R. (1982) The influence of testosterone on neuromuscular transmission in hormone sensitive mammalian skeletal muscles. *Muscle Nerve*, **5**, 232–237.
24. Oki, K., Wiseman, R.W., Breedlove, S.M. and Jordan, C.L. (2013) Androgen receptors in muscle fibers induce rapid loss of force but not mass: implications for spinal bulbar muscular atrophy. *Muscle Nerve*, **47**, 823–834.
25. Arnold, A.P. and Gorski, R.A. (1984) Gonadal steroid induction of structural sex differences in the central nervous system. *Annu. Rev. Neurosci.*, **7**, 413–442.
26. Lanman, T.A., Bakar, D., Badders, N.M., Burke, A., Kokkinis, A., Shrader, J.A., Joe, G.O., Schindler, A.B., Bott, L.C., Harmison, G.G. *et al.* (2016) Sexual reassignment fails to prevent kennedy's disease. *J. Neuromuscul. Dis.*, **3**, 121–125.
27. Korber, C. and Kuner, T. (2016) Molecular machines regulating the release probability of synaptic vesicles at the active zone. *Front Synaptic Neurosci.*, **8**, 1–17.
28. Dolphin, A.C. (2012) Calcium channel auxiliary alpha2delta and beta subunits: trafficking and one step beyond. *Nat. Rev. Neurosci.*, **13**, 542–555.
29. Calloway, N., Gouzer, G., Xue, M. and Ryan, T.A. (2015) The active-zone protein Munc13 controls the use-dependence of presynaptic voltage-gated calcium channels. *Elife*, **4**, 1–15.
30. Miki, T., Hirai, H. and Takahashi, T. (2013) Activity-dependent neurotrophin signaling underlies developmental switch of Ca2+ channel subtypes mediating neurotransmitter release. *J. Neurosci.*, **33**, 18755–18763.
31. Halievski, K., Henley, C.L., Domino, L., Poort, J.E., Fu, M., Katsuno, M., Adachi, H., Sobue, G., Breedlove, S.M. and Jordan, C.L. (2015) Androgen-dependent loss of muscle BDNF mRNA in two mouse models of SBMA. *Exp. Neurol.*, **269**, 224–232.
32. Yamamoto, L.A., Lapa, A.J. and Souccar, C. (1994) Prejunctional regulatory actions of androgens on a hormone sensitive muscle. *Muscle Nerve*, **17**, 906–912.
33. Nudler, S.I., Pagani, M.R., Urbano, F.J., McEnery, M.W. and Uchitel, O.D. (2005) Testosterone modulates Ca(v2.2) calcium channels' functional expression at rat levator ani neuromuscular junction. *Neuroscience*, **134**, 817–826.
34. Nedelsky, N.B., Pennuto, M., Smith, R.B., Palazzolo, I., Moore, J., Nie, Z., Neale, G. and Taylor, J.P. (2010) Native functions of the androgen receptor are essential to pathogenesis in a Drosophila model of spinobulbar muscular atrophy. *Neuron*, **67**, 936–952.
35. Lenman, J.A. (1965) Effect of denervation on the resting membrane potential of healthy and dystrophic muscle. *J. Neurol. Neurosurg. Psychiatry*, **28**, 525–528.
36. Weinstein, S.P. (1980) A comparative electrophysiological study of motor end-plate diseased skeletal muscle in the mouse. *J. Physiol.*, **307**, 453–464.
37. Lawson, K. (2000) Potassium channel openers as potential therapeutic weapons in ion channel disease. *Kidney Int.*, **57**, 838–845.
38. Maqoud, F., Cetrone, M., Mele, A. and Tricarico, D. (2017) Molecular structure and function of big calcium-activated potassium channels in skeletal muscle: pharmacological perspectives. *Physiol. Genomics*, **49**, 306–317.
39. Tricarico, D. and Camerino, D.C. (2011) Recent advances in the pathogenesis and drug action in periodic paralyses and related channelopathies. *Front Pharmacol.*, **2**, 1–8.
40. Tricarico, D., Mele, A., Camerino, G.M., Bottinelli, R., Brocca, L., Frigeri, A., Svelto, M., George, A.L., Jr. and Camerino, D.C. (2010) The KATP channel is a molecular sensor of atrophy in skeletal muscle. *J. Physiol.*, **588**, 773–784.
41. Tricarico, D., Montanari, L. and Conte Camerino, D. (2003) Involvement of 3Na+/2K+ ATP-ase and Pi-3 kinase in the response of skeletal muscle ATP-sensitive K+ channels to insulin. *Neuromuscul. Disord.*, **13**, 712–719.
42. Sansone, V.A., Burge, J., McDermott, M.P., Smith, P.C., Herr, B., Tawil, R., Pandya, S., Kissel, J., Ciafaloni, E., Shieh, P.

et al. (2016) Randomized, placebo-controlled trials of dichlorphenamide in periodic paralysis. *Neurology*, **86**, 1408–1416.
43. Ng, F., Lee, D.C., Schrumpf, L.A., Mazurek, M.E., Lee Lo, V., Gill, S.K. and Maselli, R.A. (2017) Effect of 3,4-diaminopyridine at the murine neuromuscular junction. *Muscle Nerve*, **55**, 223–231.
44. Quartel, A., Turbeville, S. and Lounsbury, D. (2010) Current therapy for Lambert-Eaton myasthenic syndrome: development of 3, 4-diaminopyridine phosphate salt as first-line symptomatic treatment. *Curr. Med. Res. Opin.*, **26**, 1363–1375.
45. Ionno, M., Moyer, M., Pollarine, J. and van Lunteren, E. (2008) Inotropic effects of the K+ channel blocker 3,4-diaminopyridine on fatigued diaphragm muscle. *Respir. Physiol. Neurobiol.*, **160**, 45–53.
46. Wadman, R.I., Vrancken, A.F., van den Berg, L.H. and van der Pol, W.L. (2012) Dysfunction of the neuromuscular junction in spinal muscular atrophy types 2 and 3. *Neurology*, **79**, 2050–2055.
47. Johansen, J.A., Troxell-Smith, S.M., Yu, Z., Mo, K., Monks, D.A., Lieberman, A.P., Breedlove, S.M. and Jordan, C.L. (2011) Prenatal flutamide enhances survival in a myogenic mouse model of spinal bulbar muscular atrophy. *Neurodegener. Dis.*, **8**, 25–34.
48. Martin, A.R. (1976) The effect of membrane capacitance on non-linear summation of synaptic potentials. *J. Theor. Biol.*, **59**, 179–187.
49. McLachlan, E.M. and Martin, A.R. (1981) Non-linear summation of end-plate potentials in the frog and mouse. *J. Physiol.*, **311**, 307–324.
50. Yang, L., Wang, B., Long, C., Wu, G. and Zheng, H. (2007) Increased asynchronous release and aberrant calcium channel activation in amyloid precursor protein deficient neuromuscular synapses. *Neuroscience*, **149**, 768–778.
51. Elmqvist, D. and Quastel, D.M. (1965) A quantitative study of end-plate potentials in isolated human muscle. *J. Physiol.*, **178**, 505–529.
52. Ruiz, R., Cano, R., Casanas, J.J., Gaffield, M.A., Betz, W.J. and Tabares, L. (2011) Active zones and the readily releasable pool of synaptic vesicles at the neuromuscular junction of the mouse. *J. Neurosci.*, **31**, 2000–2008.
53. Samigullin, D., Bill, C.A., Coleman, W.L. and Bykhovskaia, M. (2004) Regulation of transmitter release by synapsin II in mouse motor terminals. *J. Physiol.*, **561**, 149–158.
54. Pfaffl, M.W., Horgan, G.W. and Dempfle, L. (2002) Relative expression software tool (REST) for group-wise comparison and statistical analysis of relative expression results in real-time PCR. *Nucleic Acids Res.*, **30**, 36e–310.